Deformation and Alteration Associated With Oceanic and Continental Detachment Fault Systems: Are They Similar?

Barbara E. John and Michael J. Cheadle

Department of Geology and Geophysics, University of Wyoming, Laramie, Wyoming, USA

Detachment faults and their associated core complexes occur both in continental rifts and at mid-oceanic ridges, and represent a fundamental mode of crustal extension. Both continental and oceanic detachment faults are characterized by corrugated, domal topography; exposures of the fault surface extend tens of kilometers in the downdip direction, with dips ≤20°. In each system, the faults comprise a network of anastomosing fault zones, consisting of mylonite, cataclasite, and gouge 1– to >200 m thick, exhibiting a progressive down-temperature continuum in deformation. Both form at strain rates ~10^{-12}–10^{-14} s^{-1} and accommodate asymmetric extension. Despite these similarities, the two systems exhibit significant differences, controlled by their environments of formation. Oceanic core complexes form in thinner lithosphere, with higher geothermal gradients, dominated by olivine and feldspar rheology. In contrast, deformation in the continents is controlled by quartz and feldspar. Mylonitic rocks are predicted to be rare in oceanic core complexes and relatively common in continental core complexes. Oceanic detachment faults have a more intimate association with magmatic accretion. Hydrothermal circulation and the consequent alteration are more pronounced in oceanic detachment faults, and dominate the low-temperature fault evolution. Oceanic detachment faults are rolling-hinge-type normal faults. In contrast, some continental detachment faults initiated at a low angle (dips ≤20°). Detachment faults cutting oceanic lithosphere are nonconservative; footwalls are much more extensive than the hanging wall of the fault. Beneath continental core complexes, lower crustal flow maintains crustal thickness despite significant extension. Lower crustal flow beneath oceanic core complexes is limited and restricted to the environs of the magma chamber.

1. INTRODUCTION

For the past 30 years, there has been increasing recognition that large offset, normal-slip low-angle faults are an important component of extensional terrains, although their origin has remained controversial. In particular, there has been much discussion about the mechanical (and earthquake) paradox of slip along low-angle normal faults [i.e., *Anderson*, 1942; *Sibson*, 1985; *Axen*, 2004]. Do present-day low-angle normal faults slip at a high angle and subsequently rotate to gentle dips either as multiple high-angle faults that rotated as "dominos" [*Proffett*, 1977; *Davis*, 1983; *Jackson and White*, 1989; *Collettini and Sibson*, 2001], or by a "rolling hinge"

Diversity of Hydrothermal Systems on Slow Spreading Ocean Ridges
Geophysical Monograph Series 188

10.1029/2008GM000772

mechanism [*Buck*, 1988; *Wernicke and Axen*, 1988]; or do they initiate and slip in the brittle crust as primary low-angle structures [*John*, 1987a; *Miller and John*, 1988; *Wernicke*, 1995; *Abers*, 2001; *Numelin et al.*, 2007a]?

Large fault slip and consequent unloading leads to flexure and isostatic rebound of the footwall [*Spencer*, 1984; *Buck*, 1988]. As a result, low-angle normal faults commonly exhibit a broad, doubly plunging or domal geometry, bounding a core of metamorphic and igneous rocks. The definition originally applied to exposures in the North American Cordillera characterizes a "core complex" as a footwall of generally heterogeneous, older metamorphic-plutonic basement, overprinted by subhorizontal, lineated and foliated mylonitic and gneissic fabrics [*Davis and Coney*, 1979; *Crittenden et al.*, 1980]. A decollement or detachment fault separates the footwall and hanging wall across a steep metamorphic gradient, with brecciation and shear sense indicators implying normal-sense slip. Upper crustal, hanging wall rocks are commonly highly extended by numerous normal faults. Many continental metamorphic core complexes and associated detachment fault systems have been identified throughout a discontinuous, >3000-km-long belt extending from Mexico into Canada [*Armstrong*, 1982], with analogous structures reported in all major orogenic belts [*Wernicke*, 1995; *Burchfiel et al.*, 1992] and intracratonic rifts globally [e.g., *Colletta et al.*, 1988; *Cochran*, 2005; *Talbot and Ghebreab*, 1997; *Abers*, 2001] (Figure 1).

During the 1990s, *Cann et al.* [1997] and *Tucholke et al.* [1998] recognized analogous features to continental core complexes at mid-ocean ridges and termed them oceanic core complexes. These structures have, to date, been recognized along some intermediate, and all slow and ultraslow spreading ridges with the exception of the Gakkel Ridge [*Tucholke et al.*, 2008] (Figure 1). *Smith et al.* [2008] have argued that oceanic core complexes are a significant component of oceanic crust at mid-ocean ridges, comprising up to 60% of the seafloor along segments of the Mid-Atlantic Ridge (MAR). The recognition that tectonic extension may accommodate a large percentage of plate separation at ridges with significantly reduced magmatism [e.g., *Buck et al.*, 2005], implies that large offset low-angle normal faults may be very common at amagmatic ridges. Indeed, *Schroeder et al.* [2007] has suggested that large tracts of the seafloor at 15°N on the MAR consists of ridges defined primarily by low-angle normal faults with offsets of ~5–10 km. This interpretation is consistent with the exposure of mantle peridotite by the smooth bathymetry observed by *Michael et al.* [2003] on segments of the Gakkel Ridge and by *Cannat et al.* [2006] along the eastern Southwest Indian Ridge (SWIR). These relations led *Cannat et al.* [2006] and *Schroeder and Cheadle* [2007] to suggest two end-member styles of low-angle normal faulting at mid-ocean ridges; those that bound corrugated, domal core complexes and those that define the smooth topography along magma-starved ridges. Although much less easily accessed than continental detachment faults, significant sampling has been carried out on several detachment faults/core complexes along the MAR including Atlantis Massif at 30°N [*Blackman et al.*, 1998, 2004; *Schroeder and John*, 2004; *Blackman et al.*, 2006; *Boschi et al.*, 2006; *Karson et al.*, 2006], at 15°45′N [*MacLeod et al.*, 2002; *Escartín et al.*, 2003; *Kelemen et al.*, 2004, 2007; *Schroeder et al.*, 2007], and at 23°N/Kane [*Agar and Lloyd*, 1997; *Hansen*, 2007; *Dick et al.*, 2008], at Atlantis Bank on the SWIR [*Cannat et al.*, 1991; *Dick et al.*, 1991, 2000b; *Mehl and Hirth*, 2008; *Miranda and John*, 2010], and at the Godzilla mullion along the Parece Vela Rift, in the Philippine Sea [*Ohara et al.*, 2001; *Harigane et al.*, 2008]. These localities provide direct insight into the nature of the detachment fault/shear zone itself and enable comparisons with those from continental detachment fault systems.

Despite similarities, the most important differences between continental and oceanic detachment fault systems are the composition and therefore rheology of the rocks they deform, and the prevalence of hydrothermal activity. In continental settings, detachment faults associated with core complex formation commonly deform carbonate and quartz-rich sedimentary rocks, and locally expose quartzofeldspathic basement. The footwall may exhibit extensive hydrothermal alteration, locally hosting base-metal sulfide and barite deposits. But hydrothermal activity is less well developed compared to oceanic core complexes, is mainly focused along the detachment fault, and is associated with high angle faults in the hanging wall. In contrast, detachment faults associated with oceanic core complexes involve rheologically "stronger" gabbro and peridotite [*Agar*, 1994]. Hence, the plastic to brittle transition (under dry conditions) occurs at different pressure and temperatures compared to the same behavior in continental detachment faults. Further, the effect of seawater circulation on highly reactive olivine-bearing rocks can fundamentally affect the rheology of the fault zone [*Escartin et al.*, 1997; *Reinen*, 2000]. This interaction of seawater with exposed peridotite in the footwall is part of an incompletely understood, but possibly significant, influence on global geochemical fluxes between the lithosphere and oceans by way of hydrothermal circulation.

The identification of core complexes at mid-ocean ridges has led to broadening the definition to encompass domal exposures of middle to lower crust (±upper mantle) rimmed by low-angle normal or detachment faults. Subsequent recognition of now subhorizontal normal faults along continental margins [e.g., *Lister et al.*, 1991; *Froiztheim and Manatschal*, 1996; *Perez-Gussinye and Reston*, 2001;

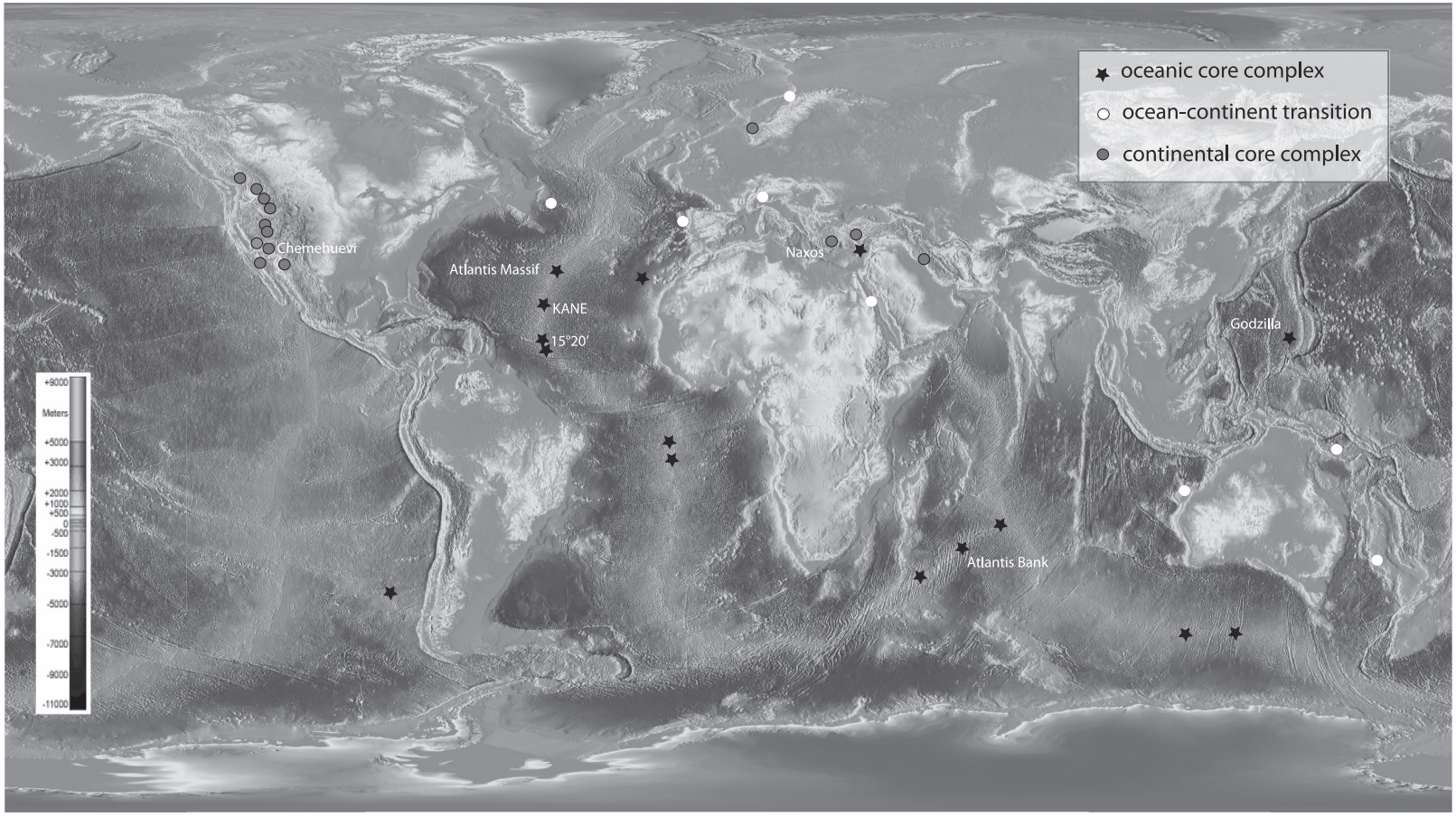

Figure 1. Global topography and bathymetric map showing the distribution of modern and ancient continental and oceanic core complexes and recognized detachment faults associated with rifted continental margins (continent-ocean transition).

Hopkinson et al., 2004] further extended the role of low-angle normal or detachment faults in stretching the lithosphere (on the continents, along mid-ocean ridges and associated with the breakup/rifting of continents and development of passive continental margins, see Figure 1). Here we review similarities (and differences) in the structural and thermal architecture of continental and oceanic core complexes. We briefly present characteristics of detachment faults in both environments, compare the structural evolution of each fault system, including the character of fault zone evolution and thickness, and recorded history of fluid flow. We end by discussing the differences between continental and oceanic detachment faults and highlight their variable rheology and longevity (10–15 Ma versus 1–3 Ma), while sharing similar strain rates.

2. NATURE OF DETACHMENT FAULT ZONES

Footwall structures formed during extension typically exhibit a deformation sequence that records strain at progressively lower pressures and temperatures due to tectonic denudation. In continental settings, this spectrum recorded in quartzo-feldspathic rocks is inferred to range from granulite and amphibolite facies metamorphism with regions of anatexis/partial melting and associated ductile fabric development, to subgreenschist facies cataclastic deformation [e.g., *Howard*, 1980; *Davis et al.*, 1980; *John*, 1987a; *Buick*, 1991; *John and Howard*, 1995; *Little et al.*, 2007; *Teyssier et al.*, 2005]. Brittle (and seismic?) tectonic unroofing of a metamorphic core complex, along now low-angle normal faults, leads to a clear continuum from penetrative high-temperature deformation to surficial normal faulting.

In the marine environment, the few studies of fault rocks associated with core complex evolution show a similar progression from granulite facies ductile deformation with possible associated magmatic deformation, overprinted down-temperature by amphibolite facies ductile deformation, to greenschist and subgreenschist facies cataclasis [*Dick et al.*, 2000b; *MacLeod et al.*, 2002; *Schroeder and John*, 2004; *John et al.*, 2004; *Boschi et al.*, 2006; *Escartín et al.*, 2003; *Miranda*, 2006; *Hansen*, 2007; *Harigane et al.*, 2008; *Mehl and Hirth*, 2008].

2.1. Continental Settings

2.1.1. Size, occurrence, and lithology. Continental core complexes and associated low-angle normal faults, originally defined based on exposures in the hinterland of the Cordilleran fold and thrust belt in western North America [*Armstrong*, 1972; *Crittenden et al.*, 1980], are now recognized globally throughout geologic time and from all tectonic settings. The footwalls are exposed over hundreds of square kilometers and up to 10's km downdip in the slip direction (Figure 2). Bounding detachment faults are characterized by a low regional dip (≤20°), are shown to accommodate up to tens of kilometers of slip [*Howard and John*, 1987; *Lister and Davis*, 1989], and often comprise networks of anastomosing fault zones, hosting fault rocks, with a down-temperature deformation history [*John*, 1987a].

Footwall rocks exposed in continental core complexes vary in composition, metamorphic grade, and preexisting fabric from stratified sedimentary rocks including carbonate and sandstone/quartzite (e.g., Snake Range, Nevada) [*Miller et al.*, 1999], heterogeneously deformed quartzo-feldspathic basement including gneiss and granite (e.g., Anatolia, Turkey [*Whitney et al.*, 2007]; Canadian Cordillera [*Teyssier et al.*, 2005]; Whipple and Chemehuevi mountains, California and Arizona [*Davis et al.*, 1980; *John*, 1987a]), syntectonic plutonic rocks, ranging in composition from mafic diorite/gabbro to evolved granite/granodiorite [e.g., *Reynolds*, 1985; *Lister and Baldwin*, 1993; *Hill et al.*, 1995; *Campbell-Stone et al.*, 2000; *Spell et al.*, 2000], or some combination of all of these (e.g., Ruby Mountains, Nevada) [*Howard*, 1980, 2003]. Because of this diverse range in rock type, preexisting fabric, thermal structure and rheology, continental core complexes, and their associated detachment fault systems vary significantly.

To facilitate a useful comparison of continental and oceanic detachment faults, we limit our discussion to the architecture and evolution of continental core complexes with footwall rocks comprising quartzo-feldspathic basement and/or syntectonic plutonic rocks with little preexisting deformation fabric. We chose not to discuss continental systems that largely occur in sedimentary rocks, and/or those that may reactivate preexisting structures, as neither of these occur in oceanic lithosphere. Our discussion is based on two examples: the Chemehuevi-Sacramento detachment fault system exposed in the Colorado River extensional corridor (CREC) California and Arizona that demonstrates the structure of a continental detachment fault system to structural depths of ≤10 km under a low to moderate geothermal gradient and the detachment fault system exposed on the island of Naxos (Greece), which exhibits higher temperature deformation and contemporaneous magmatism associated with a high geothermal gradient.

2.1.2. Deformation: Shear/fault zone thickness and associated fault rocks. For well-exposed continental core complexes in crystalline basement displaying asymmetric stretching, the spatial distribution of extensional strain associated with regional detachment systems varies in the downdip direction; it is least at the headwall, in the breakaway region (<10%)

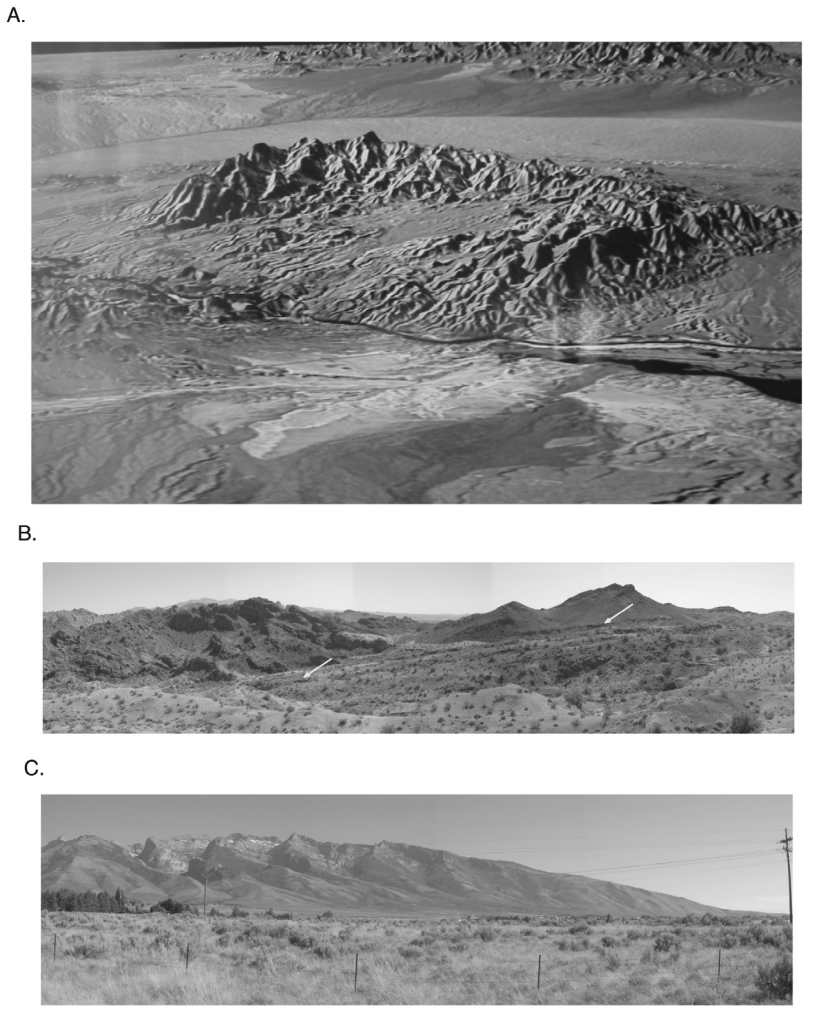

Figure 2. Regional-scale topography associated with continental core complexes. (a) Perspective Landsat image (view SSW) of the Chemehuevi Mountains core complex (California and Arizona), emphasizing the broadscale, NE-trending corrugations of the detachment fault. Footwall rocks make up the high topography, surrounded by gentle surfaces comprising hanging wall rocks. High ridges in the foreground and background are separated by ~14 km. (b) Panorama of the gently east dipping Chemehuevi detachment fault (view SE). Hanging wall blocks and erosional klippe (browns) are separated along the planar Chemehuevi fault from Cretaceous (light gray) granitoids. Arrows indicate resistant, silicified microbreccia exposed beneath the fault. Foreground ~1 km across. (c) Panorama of the eroded Ruby Mountains core complex footwall (Nevada) emphasizing the domal geometry of the fault system (view SE of the western Ruby Mountains, middle distance ~15 km across).

and increases to up to hundreds of percent in the central or core complex region, diminishing again in the slip direction, as the fault system dives below the termination [*Wernicke*, 1981; *Howard and John*, 1987]. Hanging wall rocks above the regional detachment are distended by innumerable high-angle normal faults that rotate to more gentle dips through time and together accommodate up to hundreds of percent upper to middle crustal extension.

The damage zones and fault rocks related to continental detachments are typically asymmetric, with a far greater thickness developed in the footwall relative to the hanging wall (Figure 3). Fault rocks produced by slip include gouge, breccia and cataclasite, rare pseudotachylite, and locally greenschist- to amphibolite-facies mylonitic rocks (Figures 3 and 4). The thickness and intensity of plastic and/or brittle deformation depends on the magnitude and longevity of slip,

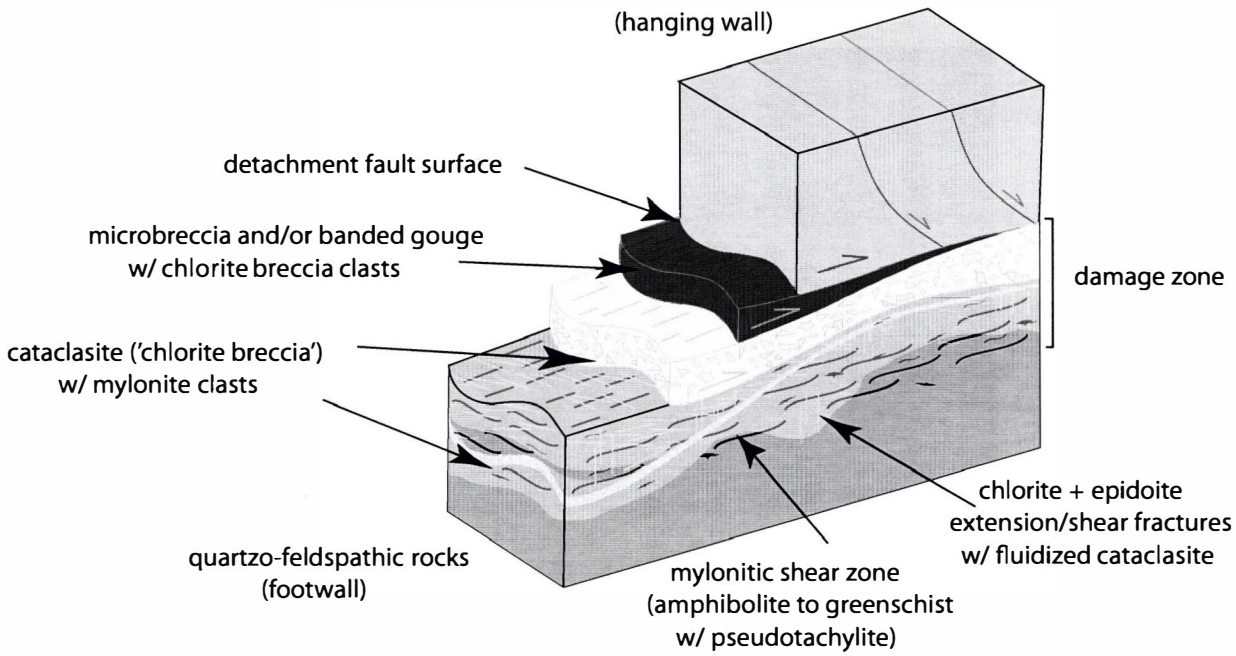

Figure 3. Architecture and evolution of continental detachment faults cutting isotropic quartzo-feldspathic basement. The fault zone comprises anastomosing low-angle normal faults/shear zones; with progressive slip, overprinting relations indicate strain localization. Hydrothermal alteration of the footwall is concentrated in the damage zone, and varies in thickness from centimeters to hundreds of meters.

proximity to the breakaway region, and relative position on the fault corrugations. Detachment faults with quartzo-feldspathic rocks in their footwall are typically marked by coherent cataclasites composed of quartz, plagioclase, and potassium feldspar (the milled-down wallrock equivalent), with retrograde minerals including chlorite ± albite ± epidote ± clinozoisite ± sericite ± actinolite and rare calcite [*Davis et al.*, 1980; *Reynolds and Lister*, 1987; *John*, 1987a; *Lister and Davis*, 1989]. In these settings, brittle deformation and fluid circulation accompany late slip on detachment faults, forming aphanitic cataclasite/ultracataclasite and/or banded gouge at the slip surface with chlorite breccia below. The aphanitic and locally silicified ultracataclasites vary in thickness from <1 to >50 cm, and lie directly beneath the detachment surface [*John*, 1987a; *Morrison and Anderson*, 1998].

2.1.2.1. High-temperature architecture of fault zones. The detachment fault system exposed on the island of Naxos (Greece) highlights the evolution of continental core complexes in regions with contemporaneous magmatism and extension. Preserved fault rocks associated with the Naxos detachment fault provide a more complete spectrum of rock fabrics and metamorphic grade than demonstrably associated with extension in most Cordilleran metamorphic core complexes [*John and Howard*, 1995]. Fault rocks show upper amphibolite facies ductile deformation with associated partial melting, pseudotachylite formation and subgreenschist facies cataclastic deformation. The clear continuum, from penetrative high-temperature deformation to pseudotachylite formation, surficial normal faulting, and conglomerate deposition, records brittle and seismic/tectonic denudation of the footwall [*John and Howard*, 1995].

Roughly 500 m structurally beneath the gently (5°–10°) north dipping Naxos detachment fault, a syntectonic granodiorite exposed in western Naxos [*Jansen and Schuiling*, 1976; *Buick and Holland*, 1989] shows a high-temperature magmatic fabric, and no evidence of subsolidus deformation. Anastomosing zones, 2–10 cm thick, of protomylonite, mylonite, and rarely ultramylonite are abundant at structural depths <400 m beneath the detachment fault surface. Microstructures associated with development of the mylonitic rocks imply temperatures between ~300° and 450°C. Veins of pseudotachylite (friction melt) and fluidized(?) cataclasite cut the granodiorite and associated mylonitic fabrics and are concentrated within the upper 200 m of the footwall. The pseudotachylite locally comprises up to 1–5 vol % of a zone 10–15 m thick [*John and Howard*, 1995]. Rarely, pseudo-

tachylite veins show a lineated mylonitic overprint, in turn cut by down-to-the-north brittle normal faults. This relationship is characteristic of mixed mode deformation and implies that the granodiorite in the footwall to the Naxos detachment system alternated from the plastic to the semibrittle field, with flow occurring during interseismic periods, mixed with coseismic slip during earthquakes [*Sibson*, 1977; *Scholz*, 2002].

Anastomosing zones of chlorite- and epidote-rich cataclasite up to 1 m thick within the upper 100 to 200 m of the granodiorite strike roughly orthogonal to the mylonitic lineation. Cross-cutting chlorite-filled joints and quartz veins indicate repeated periods of jointing, fluid flow, and vein fill, followed by additional joint formation. Cataclasis, brecciation, and retrograde chlorite and limonite alteration increase in intensity toward the contact with the hanging wall and locally obliterate the preexisting mylonitic fabric. Less than 10 m below the Naxos detachment fault, the granodiorite is characterized by intense fracturing and bleaching and, locally, by clay-rich gouge and breccia dominated by hematite and limonite alteration assemblages. Along the entire northern coast of Naxos, breccia and cataclasite ≥100 m thick, crop out subparallel to the Naxos detachment fault surface where exposed.

2.1.2.2. Low-temperature architecture of fault zones. The low temperature architecture of continental detachment faults within the brittle crust (<10 km) is well expressed by the Cenozoic normal fault system exposed in the CREC [*Howard and John*, 1987] at the latitude of the Chemehuevi and adjacent Sacramento Mountains, California and Arizona [*John*, 1987a, 1987b; *Campbell-Stone et al.*, 2000; *Campbell-Stone and John*, 2002]. The mapped fault geometry, associated fault rocks, detailed thermochronometry, and inferred evolution of the fault system place tight constraints on the fault initiation angle and the process of crustal attenuation.

Extreme extension involving the upper and middle crust over hundreds of square kilometers in the central CREC (Chemehuevi and Sacramento mountains) was accomplished along a stacked, anastomosing sequence of brittle, NE dipping low-angle normal faults discordantly cutting deformed Proterozoic and Mesozoic crystalline basement, and Miocene intrusive rocks. The large-displacement (>18 km) Chemehuevi-Sacramento detachment fault separates hanging wall and footwall rocks, and juxtapose rocks from different crustal depths [*John*, 1987a]. Hanging wall rocks were distended by innumerable high-angle normal faults that rotated to more gentle dips through time, and together, accommodated up to ~100% extension regionally [*Howard and John*, 1987]. These faults have tens to hundreds of meters separation, but are nowhere known to cut the regional detachment fault. In contrast to Naxos, the footwall to the detachment fault system is underlain by few rocks that have undergone plastic deformation during extension (Figure 4), apart from thin, semibrittle shear zones exposed in the structurally deepest portions of the footwall [*John*, 1987a, 1987b]. The absence of significant, temporally related mylonite implies deformation within the brittle, seismogenic regime. The youngest fault is demonstrably the regionally developed detachment, precluding the possibility of significant rotations of present-day low-angle normal faults to their gently dipping orientation by younger higher angle fault.

The footwall to the detachment system includes the structurally deepest rocks exposed, below the small-displacement (≤2 km) Mohave Wash fault [*John*, 1987a, 1987b]. This fault is structurally overlain and cut by the regionally developed, large-displacement (≥18 km) Chemehuevi detachment fault, which is, in turn, overlain by the Devils Elbow fault. The two structurally deepest faults are exposed for a distance of >23 km in the original slip direction. The Mohave Wash fault is exposed continuously as a sinuous trace over >350 km^2, and at outcrop scale, damage zones associated with each fault are roughly planar, but viewed at map scale, both the Mohave Wash and Chemehuevi faults are corrugated parallel to the documented slip direction. The wavelengths of the corrugations range between 200 m and 10 km, and amplitude from 20 to 400 m [*John*, 1987a]. Dips on each detachment fault therefore vary from horizontal or very gently inclined along the troughs or crests of the corrugations, to as much as 40° perpendicular to the slip direction on the steeper flanks of the corrugations (Figure 3). Orthogonal to, and superimposed on, these corrugations are broad synformal-antiformal undulations of the fault surface likely due to isostatic rebound.

Rocks produced by slip on the detachment fault in the Chemehuevi Mountains area include gouge, breccia, rocks of the cataclasite series, and only rare protomylonite and pseudotachylite. Damage zone thickness varies with relative position on corrugations from less than 2 m near the crests of the corrugations, to more than 100 m along trough walls. Retrograde mineral assemblages are consistently greenschist and subgreenschist grade (e.g., chlorite, epidote, albite, clinozoisite, sericite, actinolite, and calcite). The structurally deepest exposures show evidence of reworking of these fault rocks at shallower structural levels to form gouge and breccia rich in hematite, calcite, and/or clay (illite and smectite) that overprint preexisting cataclasite. Rare veins of pseudotachylite a few millimeters to centimeters thick and up to 0.5 m long are locally recognized adjacent to the Mohave Wash fault. Thin mylonites 0.01–1 m thick are present, but no major zones of plastic deformation are directly attributed to detachment faulting [*John*, 1987a]. The most recent slip surfaces crop out as planar zones, marked in the deepest levels

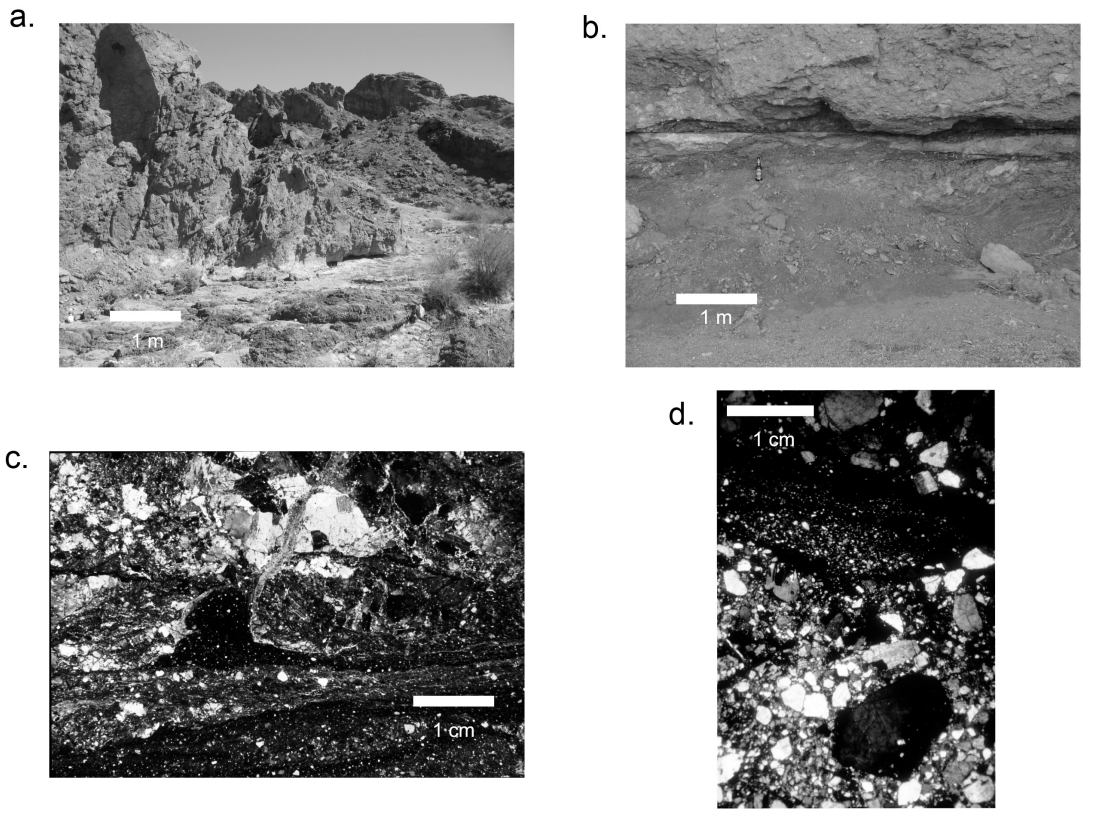

Figure 4. Macrostructural and microstructural character of continental detachment fault zones and associated fault rocks. (a) Exposure of Chemehuevi detachment fault, near Devils Elbow, California. The fault juxtaposes a hanging wall of hydrothermally altered Proterozoic granite (dark gray) against the footwall of Cretaceous granitoid (light gray). The fault zone comprises hydrothermally altered cataclasite, with a thin layer of banded, clay gouge at the slip surface. (b) Sacramento detachment fault juxtaposing syntectonic alluvial fan deposits in the hanging wall, against Miocene granitoids in the footwall. The fault zone is characterized by banded clay gouge, with centimeter-scale folds indicating top-NE normal-sense movement. (c) Pseudotachylite vein hosted by cataclasite derived from Cretaceous granite, associated with the small displacement (<2 km slip) Mohave Wash fault (south-central Chemehuevi Mountains). (d) Layered granitic breccia, with hematite cement (Chemehuevi detachment fault, central Chemehuevi Mountains).

exposed by the juxtaposition of hematite- and clay-rich gouge and breccia, against chlorite- and epidote-rich cataclasite (Figures 3 and 4). Locally, flow-laminated gouge and breccia up to 1 m thick are preserved in synformal hinges of the faults. These relations imply that the Chemehuevi fault evolved from a thick zone of cataclasite to a thinner zone of breccia, to a sharp planar discontinuity marked by breccia and gouge locally, consistent with strain localization within the upper crust.

2.1.3. Slip rates and strain localization. Estimated strain rates associated with slip on continental detachment faults are few, in part, because no active detachments have been recognized and monitored. Low-temperature chronometers ($^{40}Ar/^{39}Ar$, apatite fission track, and apatite and zircon (U-Th)/He) have been used instead to establish the temperature evolution of both hanging and footwall rocks associated with core complexes [*Richard et al.*, 1990; *John and Foster*, 1993; *John and Howard*, 1995; *Howard and Foster*, 1996]. Typically, ages from each chronometric technique give internally consistent results that show a systematic decrease in age of footwall rocks in the known slip direction. This decrease is interpreted to reflect the lateral passage of isotherms at the top of the footwall and can be used to estimate slip rates from the inverse slope of mineral age with distance in the slip direction. Time-averaged fault slip rates range from ~2 to 30 km Ma^{-1} (average 3–8 mm a^{-1}) [*John and Foster*, 1993; *Foster and John*, 1999; *Brady*, 2002; *Carter et*

al., 2004]. Recent detailed applications of fission track and (U-Th)/He dating of zircon and/or apatite on Naxos, Greece [*John and Howard*, 1995; *Brichau et al.*, 2006], the Harcuvar Mountains, Arizona Mountains [*Carter et al.*, 2004], and the Chemehuevi and Sacramento Mountains, California [*Carter et al.*, 2006] suggest that slip rates may vary during development of the detachment fault system, accelerating from 5 to 6 km Ma^{-1} during early motion to >13 km Ma^{-1} on Naxos, ~3 to 30 km Ma^{-1} in the Harcuvar Mountains, and 1–3 km Ma^{-1} increasing to 6 km Ma^{-1} along the Chemehuevi-Sacramento detachment fault system. Published shear/damage zone thicknesses (outlined above), combined with the estimated fault slip rates from thermochronology, imply time-averaged strain rates associated with slip on continental detachments from ~10^{-12} to 10^{-14} s^{-1}. Independently, *Campbell-Stone and John* [2002] made simplified, time-integrated strain rate estimates in the CREC at the latitude of the Sacramento Mountains based on geologic and temporal constraints. There the fastest strain rates (10^{-14} s^{-1}) occurred during both brittle failure and magmatism (regional-scale dike intrusion), comparable to strain rates estimated from the central Basin and Range province (10^{-14} to 10^{-15} s^{-1}) [*Wernicke*, 1992; *Sonder and Jones*, 1999] during the Miocene and to rates measured in active rift systems today [e.g., *Abers*, 2001; *Campbell-Stone and John*, 2002].

2.1.4. Hydrothermal alteration and evidence for fluid flow. Fluid flow in and around active normal faults results from at least two related factors: episodic change in the state of stress and fault zone permeability [*Sibson*, 2000]. Fault-rock assemblages from the denuded footwalls of major normal faults provide information on the physical and chemical conditions at depth that can be used to decipher the relationships between tectonic and hydrothermal activity [*Sibson*, 2000; *Reynolds and Lister*, 1987].

To date, there are very few studies focused on alteration and hydrothermal fluid flow associated with continental detachment faults. Field observations indicate that footwall rocks below continental detachments typically show evidence of hydrothermal circulation localized within and adjacent to the damage zone associated with each detachment fault and to minor high-angle normal and strike slip faults that cut the footwalls [*John*, 1987a, 1987b; *Reynolds and Lister*, 1987]. In all cases, alteration thickness varies from centimeters to hundreds of meters (Figure 3).

Hydrothermal circulation requires cracking and the availability of fluids; brittle fracture associated with detachment fault slip provides the fluid pathways. General models for detachment-related alteration in continental core complexes consider hanging wall-derived fluids (meteoric and/or basin brines) [*Chapin and Lindley*, 1986; *Roddy et al.*, 1988], fluids derived near the breakaway (likely similar to hanging wall fluids), and fluids associated with metamorphic and/or igneous reactions in the footwall [*Reynolds and Lister*, 1987].

Early chlorite-epidote ± calcite alteration typically occurs along (and in the footwall beneath) detachment faults cutting quartzo-feldspathic rocks forming "chlorite breccias." These cataclastic rocks locally contain base-metal sulfide and barite deposits [*Spencer and Welty*, 1986]. In the southern Basin and Range (California and Arizona), updip sections of the fault zone (formed at shallow crustal levels close to a breakaway) are characterized by hematite and limonite-altered fault rocks, whereas downdip, the chlorite breccias are cut by both massive and fracture-filling specular hematite [*John*, 1987a; *Spencer and Welty*, 1986; *Campbell-Stone et al.*, 2000]. *Morrison* [1994] showed that both mylonitic and nonmylonitic rocks in the footwall to the Whipple detachment fault interacted with surface-derived meteoric waters, indicating infiltration of meteoric fluids during juxtaposition of the footwall against the base of the faulted hanging wall. High-angle normal faults in the hanging wall served as the conduits for the downward circulation of surface-derived fluids. Regional studies of oxygen and hydrogen isotopes show that alteration associated with chlorite breccia and cataclasite developed at 300–350°C during incursion of hydrothermal fluids along detachment faults in the southern Basin and Range [*Kerrich*, 1988; *Michalski et al.*, 2007]. A detailed transect of samples collected in the footwall to the Whipple fault have quartz-epidote $\delta^{18}O$ from 4.1‰ to 6.4‰, showing a systematic increase toward the fault. These fractionations in oxygen suggest temperatures up to ~430° at 50 m below the fault, to 350°C at 12 m below, and are explained by advective heat extracted by circulation of meteoric fluids [*Morrison and Anderson*, 1998]. Meteoric fluids are therefore able to penetrate across the detachment fault into the footwall up to tens (and likely hundreds) of meters locally. A recent study coupling field observations, oxygen-isotope data, and modeling from the Shuswap core complex in British Columbia suggests that meteoric fluids were focused along a subhorizontal shear zone to depths of at least 7 km [*Person et al.*, 2007]. Fluid-rock interactions associated with this flow system resulted in oxygen isotope depletion of mylonitic rocks in a zone up to 900 m thick. On Naxos (Greece), low-temperature hydrothermal alteration of the footwall is indicated by the late, limonite-stained, clay-rich breccias up to 10 m thick, with lowered $\delta^{18}O$ values (5.9–7.2‰, relative to primary igneous values collected further from the fault, 10–11‰) [*Altherr et al.*, 1988; *John and Howard*, 1995].

In contrast, hanging wall rocks above continental detachment faults are commonly potassium (K)-metasomatized,

likely the result of either low-temperature diagenetic or high-temperature hydrothermal processes [*Kerrich*, 1988]. In the Harcuvar Mountains (AZ), oxidized basin brines metasomatized hanging wall tuff and mafic lavas into secondary K-feldspar-hematite-quartz mineralogy [*Roddy et al.*, 1988]. Primary minerals were replaced by assemblages of K-feldspar (adularia) + hematite ± clay minerals, ± quartz, although primary textures can be preserved [*Chapin and Lindley*, 1986; *Hollocher et al.*, 1994]. Fe- and Cu oxide mineralization (principally as specular and earthy hematite and chrysocolla) have associated fluid inclusions with moderate homogenization temperatures (150–350°C) and salinities of 10–23 equivalent weight percent NaCl), compatible with precipitation from connate brines. Other models for hanging wall alteration/mineralization favor shallow, oxidizing, and warm meteoric fluids [*Chapin and Lindley*, 1986; *Kerrich*, 1988; *Roddy et al.*, 1988; *Spencer and Welty*, 1986]. Mineralization along detachment faults in crystalline rocks likely occurs as metal-rich brines circulate through hanging wall rocks, come in contact with the footwall hosting significant stored heat, driving hydrothermal convection and fluid mixing [*Spencer and Welty*, 1986; *Kerrich*, 1988; *Halfkenny et al.*, 1989; *Wilkins et al.*, 1986].

2.1.5. Estimates of continental detachment fault initiation angle. Structural constraints on the initiation angle of the detachment fault system exposed in the Chemehuevi Mountains are based on fault rock type and mineral deformation mechanisms, orientation, and cross-cutting relations of syntectonic dikes and faults, and metamorphic grade of footwall rocks to the fault (Figure 5). Together, these constraints suggest that the initial dip of the Chemehuevi fault system is limited to <30° [*John*, 1987a]. Detailed thermochronometric data from the footwall rocks indicate a moderate difference in paleo-temperature across the footwall prior to the onset of extension [*John and Foster*, 1993]. Granitic rocks exposed in the SW and NE parts of the footwall were at ~100°C and ~400°C, respectively, separated by 23 km down the known slip direction. This gradual increase in temperature with depth is attributed by *John and Foster* [1993], to the gentle warping of an originally subhorizontal isothermal surface and constrains the exposed part of the Chemehuevi detachment fault to have had a regional dip initially of 5° to 25°. Complementary paleomagnetic studies in the adjacent Sacramento Mountains suggest little footwall rotation (<25°) after emplacement of syntectonic plutons exposed in the footwall [*Campbell-Stone et al.*, 2000; *Campbell-Stone and John*, 2002], limiting the initial fault dip to <30°.

Structural reconstructions indicate that many detachment faults (in addition to that exposed in the Chemehuevi Mountains), were initiated and moved at low angles, including the Whipple Mountains [*Yin and Dunn*, 1992], the Harcuvar Mountains in central Arizona [*Reynolds and Spencer*, 1985], and in the Mormon Mountains, Nevada [*Wernicke*, 1995]. Other low-angle normal faults, however, were demonstrably initiated at higher angles. Present-day low-angle normal faults exposed in the Yerington district (Nevada) were initiated with dips of 60°–70°, and rotated "domino-style" to more shallow orientations [*Proffett*, 1977]. Large fault slip and consequent removal of hanging wall rocks leads to flexure and isostatic rebound of the footwall via a "rolling hinge" [*Spencer*, 1984; *Buck*, 1988; *Wernicke and Axen*, 1988]. Although this is likely a common process, the magnitude of rotation in continental settings is generally not in excess of 10°–20° during flexural rotation [*John*, 1987a; *Axen and Bartley*, 1997].

There has been much debate about how low-angle normal-sense slip might be facilitated. High-fluid pressure in faults can lower the effective normal stress and aid slip on misoriented faults. Several authors [*John*, 1987a; *Reynolds and Lister*, 1987; *Axen and Selverstone*, 1994] have suggested that such high fluid pressures may have assisted slip along continental detachments. Evidence for fluid within the fault zones is provided by the presence of hydrous minerals (e.g., chlorite, actinolite, and mixed clay-gouge) in "chlorite breccias," and stable isotope studies suggest that large volumes of various fluids have passed through the low-angle normal fault zones [*Losh*, 1997; *Holk and Taylor*, 2007; *Morrison and Anderson*, 1998]. Additionally, the presence of weak minerals in fault zones may lower the coefficient of friction [*Byerlee*, 1978] and help enable low-angle slip. Clays are commonly associated with continental detachment fault zones [*John*, 1987a; *Cowan et al.*, 2003; *Numelin et al.*, 2007b] and, as intrinsically weak, may facilitate low-angle slip once these faults are initiated [*John*, 1987a; *Hayman et al.*, 2003; *Axen*, 2004].

The ability of wet quartz to deform by dislocation creep at temperatures of 450–500°C and differential stresses of ≤50 MPa [*Hirth et al.*, 2001] implies that continental detachment faults likely root into mylonite zones in the middle crust, consistent with the observation that quartz mylonites can form under greenschist conditions [*Behrman*, 1985] (Figure 5). Steeper geothermal gradients may lead to the formation of quartz-bearing mylonites at more shallow structural depths. The presence of dry quartz and/or a plagioclase-dominated rheology increases the temperature and stress required for dislocation creep and, thus, suppresses the field of plastic deformation [*Scholz*, 2002]. Detachment faults rooted in feldspar-rich granodiorite (such as the Chemehuevi detachment fault) may only show limited development of semi-brittle fault rocks (protomylonites), consistent with field

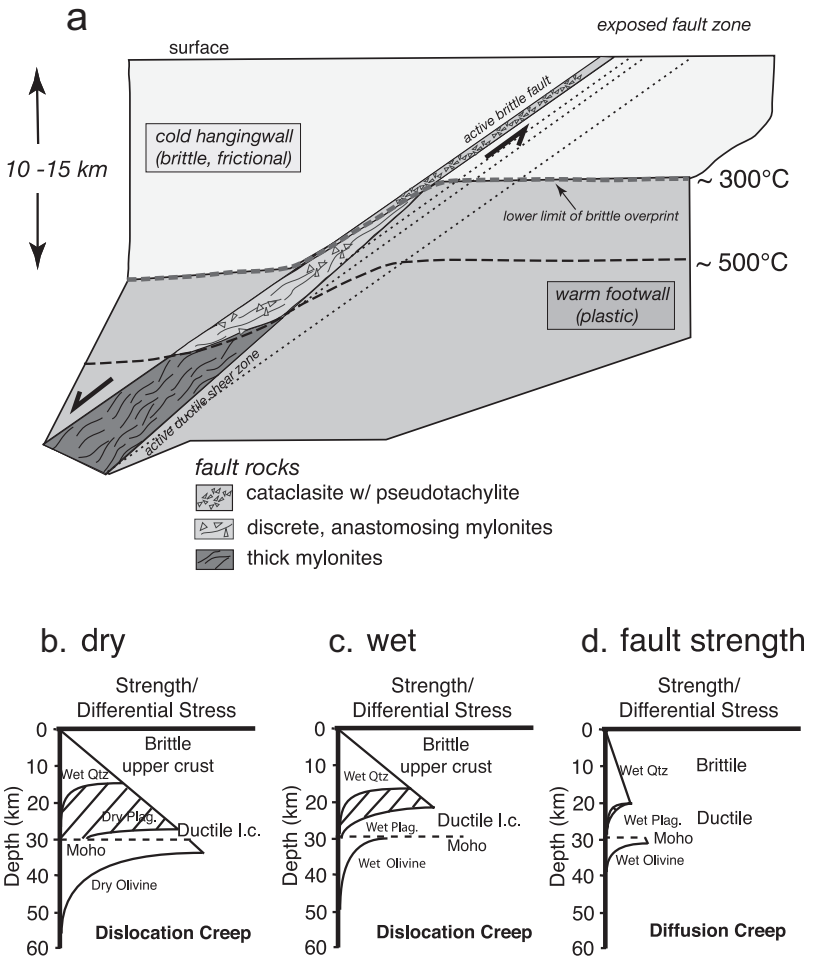

Figure 5. (a) Schematic section through a continental detachment fault system, showing strain localization with decreasing temperature. Assuming large magnitude fault slip, the surface exposure of the fault zone should show a progression from ductile to brittle deformation (modified from *Handy et al.* [2007]). Cartoon models of strength versus depth for continental crust and continental detachment faults (modified from *Burgmann and Dresen* [2008]): (b) crust and mantle dominated by the rheology of wet quartz, dry plagioclase and dry olivine, (c) crust and mantle dominated by the rheology of wet quartz, wet plagioclase and wet olivine, and (d) fault strength, assuming weakening due to reaction softening from alteration or elevated pore pressure and diffusion creep due to grain size reduction.

observations. Alteration and mineralization (including formation of clays) typically accompany detachment faulting in continental core complexes [*Wilkins et al.*, 1986], with hydrothermal fluids likely playing an important role in the faulting process [*John*, 1987a; *Reynolds and Lister*, 1987]. Although there is little evidence for any early, high-temperature infiltration of water during initiation of continental detachment faults, significant evidence exists for later involvement of fluids in altering (and likely reducing friction/weakening) the fault zone to produce clay-rich gouges and/or elevated pore fluid pressure [*John*, 1987a; *Numelin et al.*, 2007b]. The mechanics of low-angle normal faulting, however, remains enigmatic, leaving unresolved questions about fault strength and the state of stress in continental crust.

2.2. Oceanic Settings

Oceanic core complexes and their associated detachment faults are characterized by broad domes, commonly elongate parallel to the spreading direction, with pronounced flowline parallel corrugations of the surface (Figure 6) [*Dick et al.*, 1991; *Blackman et al.*, 1998; *Tucholke et al.*, 1998].

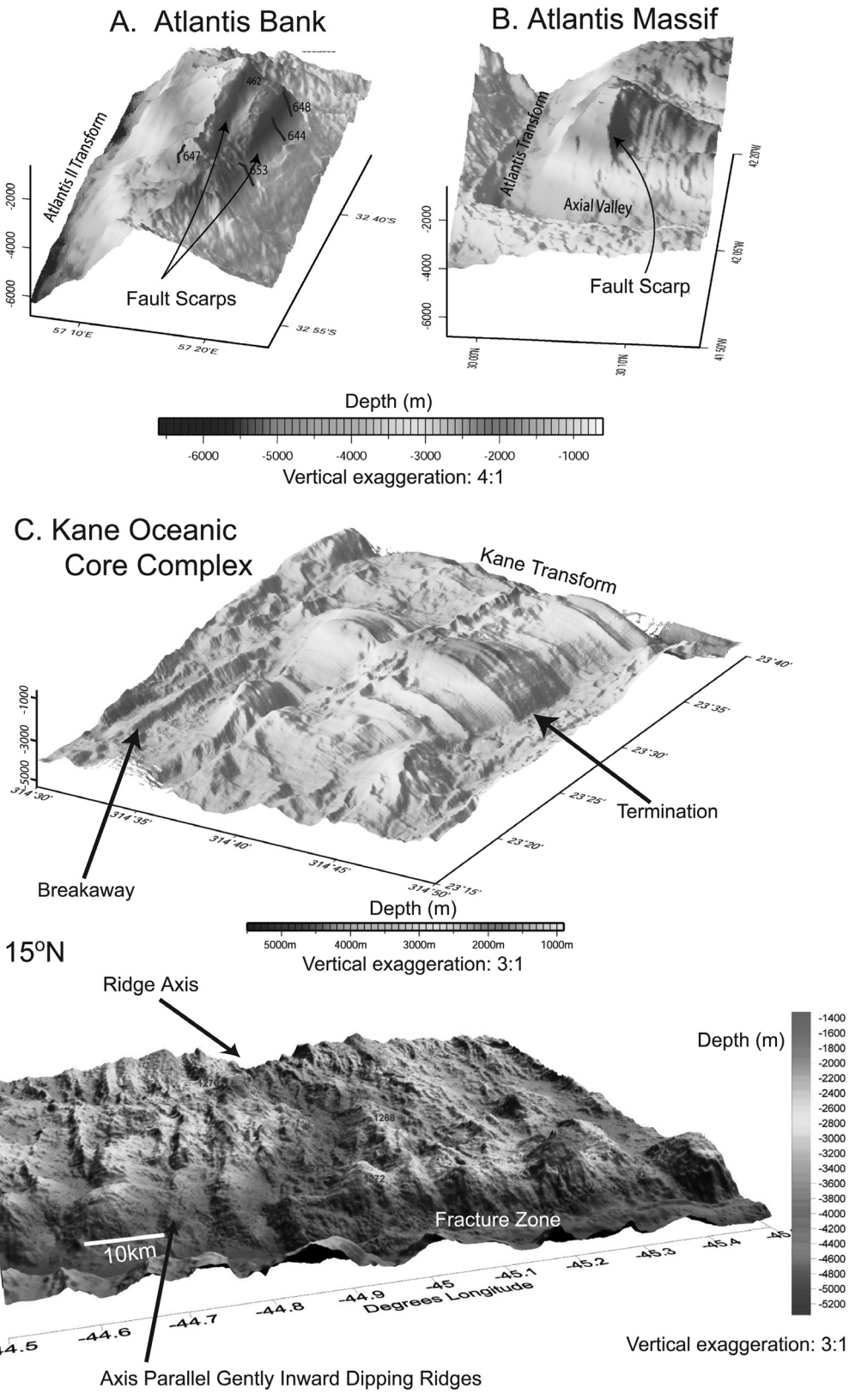
A. Atlantis Bank
462
648
644
647
653
Atlantis II Transform
Fault Scarps
-2000
-4000
-6000
57 10'E
57 20'E
32 40'S
32 55'S
B. Atlantis Massif
Atlantis Transform
Axial Valley
Fault Scarp
42.20'N
42.05'N
41.50'N
30.00'W
30.10'W
Depth (m)
-6000
-5000
-4000
-3000
-2000
-1000
Vertical exaggeration: 4:1
C. Kane Oceanic
Core Complex
Kane Transform
Termination
Breakaway
-1000
-3000
-5000
314°30'
314°35'
314°40'
314°45'
314°50'
23°40'
23°35'
23°30'
23°25'
23°20'
23°15'
Depth (m)
5000m
4000m
3000m
2000m
1000m
Vertical exaggeration: 3:1
D. 15°N
Ridge Axis
Depth (m)
-2000
-4000
1268
1272
Fracture Zone
10km
-44.5
-44.6
-44.7
-44.8
-44.9
-45
-45.1
-45.2
-45.3
-45.4
Degrees Longitude
-1400
-1600
-1800
-2000
-2200
-2400
-2600
-2800
-3000
-3200
-3400
-3600
-3800
-4000
-4200
-4400
-4600
-4800
-5000
-5200
Vertical exaggeration: 3:1
Axis Parallel Gently Inward Dipping Ridges

They are associated with elevated residual mantle Bouguer gravity anomalies (RMBA), exposure of subvolcanic lithosphere (lower crustal gabbro and/or peridotite/mantle) in their footwalls [*Tucholke et al.*, 2008], and are recognized along ultraslow, slow, and intermediate spreading ridges with full spreading rates less than ~80 mm a^{-1} [*Tucholke et al.*, 2008]. Typically, they only form on one side of the ridge axis; and thus, the ridge is structurally asymmetric [*Karson*, 1999]. Oceanic detachment faults were originally linked genetically to a position adjacent to inside corners of ridge-transform intersections [*Tucholke et al.*, 1998], but have subsequently been recognized in many slow and ultraslow spreading mid-ocean ridge settings away from transform boundaries [*Fujiwara et al.*, 2003, *Smith et al.*, 2006, 2008]. The geometry of exposed fault surfaces is well-constrained by multibeam bathymetry and sidescan sonar, but less is known about their continuation below the surface, the way in which they interact with steeper faults bounding the axial valley, and their relationship to magmatism and hydrothermal circulation.

2.2.1. Size, occurrence, and lithology. Documented exposures of oceanic detachment fault surfaces typically vary between ~15 and 32 km in the ridge-normal (downdip) direction (representing 1 to >2.5 million years of plate spreading; Figure 6), producing footwall outcrops between 100 and 400 km^2 in area [*Tucholke et al.*, 1998]. Godzilla Mullion, associated with intermediate-fast spreading in the back arc Parece Vela Basin in the Philippine Sea, is by far the largest known oceanic core complex with ~125 km of footwall exposure in the ridge-normal direction (estimated exposure of the core complex is >6000 km^2 [*Ohara et al.*, 2001; *Harigane et al.*, 2008].

The abundance of oceanic core complexes at mid-ocean ridges varies with location, likely reflecting the delicate balance between plate spreading rate, thermal gradient, and magmatic input required for their formation [*Buck et al.*, 2005; *Tucholke et al.*, 2008]. *Smith et al.* [2008] suggest that oceanic core complexes locally account for up to 60% of the seafloor at 13°N along the MAR, whereas *Cannat et al.* [2006] suggest only 4% of the seafloor of the easternmost SWIR comprises core complexes. Similarly, *Schroeder et al.* [2007] argue that only 3% of the seafloor at 15°N on the MAR comprises core complexes. Recently, *Cannat et al.* [2006] and *Schroeder et al.* [2007] independently identified "smooth" seafloor topography along the easternmost SWIR and at 15°N on the MAR characterized by elongate 10- to 20-km-wide, low-relief ridges (not domes), bound by gently inward and steeper outward dipping slopes. These ridges expose mantle peridotite and gabbro at the seafloor, may show poorly developed corrugations, and are interpreted as relatively large offset (5–10 km), low-angle normal faults. *Schroeder and Cheadle* [2007] argue that the faults that bound these ridges be considered a second type of low-angle normal fault, forming at ridges that are either amagmatic or have significantly reduced magmatism. These ridges form >35% of the seafloor on the easternmost SWIR [*Cannat et al.*, 2006] and greater than 60% of the seafloor at 15°N on the MAR [*Schroeder et al.*, 2007]. Similar ridges have been observed along amagmatic segments of the Gakkel Ridge [*Michael et al.*, 2003].

There is general consensus that oceanic detachments form at ridges where magmatism is insufficient to accommodate the full plate-spreading rate [e.g., *Tucholke et al.*, 1998; *Buck et al.*, 2005; *Schroeder et al.*, 2007; *Escartín et al.*, 2008]. This assertion is based on geologic and geophysical observations, as well as geophysical modeling. The presence of an elevated RMBA over most core complexes suggests that a normal thickness crust is not present below the footwall [*Blackman et al.*, 2004; *Tucholke et al.*, 2008] and is explained by tectonic thinning of a normal crustal section and/or reduced magmatism during core complex formation. Additional evidence for reduced magmatism is provided by erupted basalt compositions from ridge segments with detachment faults, consistent with reduced extents of partial melting and crystallization at higher pressures [*Escartín et al.*, 2008].

Detailed studies of the footwalls to oceanic core complexes are hampered by the near ubiquitous veneer of carbonate and basalt debris [e.g., *Schroeder et al.*, 2002; *Blackman et al.*, 2004; *Searle et al.*, 2003]. Most information has come from surveys along transform walls bounding core complexes [e.g., *Schroeder and John*, 2004; *Boschi et al.*, 2006], scarps exposed by ridge or transform parallel cross faults [*Dick et al.*, 2008; *Miranda*, 2006], and by shallow and deep drilling [*Escartín et al.*, 2003; *Dick et al.*, 2000b; *Kelemen et al.*, 2004; *Blackman et al.*, 2006]. These studies indicate that the footwalls comprise a mixture of mantle peridotite and gabbro, implying a "crustal" section similar to that proposed by *Cannat* [1996] for slow spread crust. The size and shape of

Figure 6. (opposite) Three-dimensional bathymetry of oceanic core complexes, and a low-angle normal fault terrain. (a) Atlantis Bank (57°E, SWIR); view is NNW. (b) Atlantis Massif (30°N, MAR), view west. (c) Kane oceanic core complex (23°N, MAR). Footwall corrugations are especially visible in the Kane and Atlantis Massif core complexes; view is NW. (d) Rift valley parallel ridges at 15°N, MAR. These ridges exhibit 5- to10-km-wide gently dipping inward facing slopes and more steeply dipping outward facing slopes; view is SSW.

the gabbroic plutons is poorly resolved, but mapping and drilling at Atlantis Bank [*Dick et al.*, 2000a; *Matsumoto et al.*, 2002; *Schwartz et al.*, 2005] suggests continuous accretion of gabbroic crust in the footwall for a minimum of 35 km parallel to spreading, with a local thickness of >1.5 km. Similarly, drilling at Atlantis Massif suggests a minimum gabbro thickness at least locally of >1400 m [*Blackman et al.*, 2006]. *Canales et al.* [2008] used two-dimension seismic tomography to map the shallow (0.5–1.4 km) seismic velocity structure of several core complexes on the MAR. Their data suggest the presence of large 10–100 km^2 gabbro bodies distributed heterogeneously in each footwall.

Observations from oceanic core complexes investigated to date suggest that gabbroic bodies are common in the center of the domes, with peridotite more common on their margins, as at Atlantis Bank, and at the southern wall of Atlantis Massif. This led *Ildefonse et al.* [2007] and *Schroeder et al.* [2007] to suggest that oceanic core complexes may be cored by gabbro plutons. *Schroeder et al.* [2007] suggest that some magmatism may lead to formation of core complexes, but very reduced magmatism may be associated with the formation of low-angle normal faults that bound long-ridge-axis parallel ridges adjacent to the MAR at 15°N, and along the SWIR [smooth terrane of *Cannat et al.*, 2006]. These suggestions are consistent with the modeling of *Tucholke et al.* [2008], which predicts that oceanic core complexes form when magmatism accounts for 30–50% of plate separation, and smaller offset, more symmetric, rotated normal faults develop when magmatism accounts <30% of plate separation. *Tucholke et al.* [2008] and *Canales et al.* [2008] further suggest that increased magmatism during core complex formation may be instrumental in terminating the detachment fault that bounds the core complex.

The relationship of contemporaneous detachment faulting and magmatism is demonstrated by cross-cutting fabric and intrusive relations in samples recovered from fault zones (Figures 7 and 8) that show overlap in time and space between deformation, magmatism, and hydrothermal alteration [*Dick et al.*, 2000b; *MacLeod et al.*, 2002; *Kelemen et al.*, 2004; *Blackman et al.*, 2006; *Hansen*, 2007; *McCaig et al.*, 2007]. Plastic and/or semibrittle fabrics, in both peridotite and gabbro, are demonstrably cut by gabbro, diabase (with glassy and/or fine-grained margins), and amphibole veins. Locally, diabase fragments are incorporated into highly sheared serpentinite [*MacLeod et al.*, 2002; *Blackman et al.*, 2006).

2.2.2. Deformation: Shear/fault zone thickness and associated fault rocks. The architecture of the faults/shear zones associated with oceanic detachments is highly variable (Figures 7 and 8). Samples collected from both high-angle fault scarps cutting the footwall and by drilling suggest that the detachment fault/shear zones can vary from meters to hundreds of meters in thickness. In detail, the detachment fault comprises anastomosing, high-strain shear/fault zones, each up to a few meters thick, separated by less-deformed zones; the spacing of the fault/shear zones increases with depth below the main fault surface. In contrast to continental detachment systems, detailed mapping of oceanic detachments is limited in 3-D, and details, such as fault rock thickness related to position on corrugations, are not resolved.

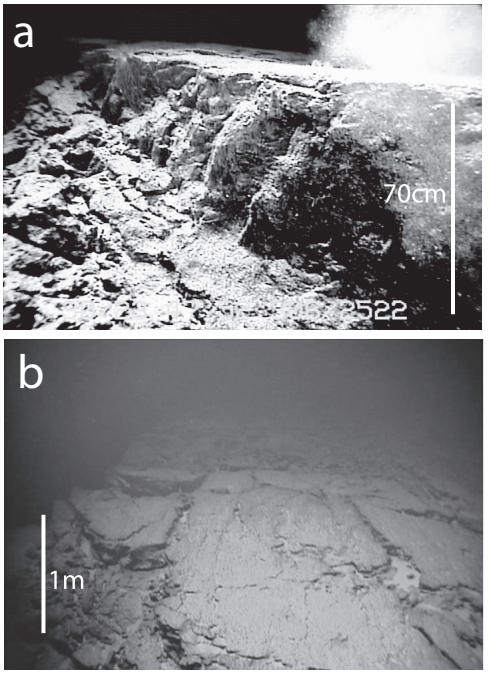

Figure 7. Photographs of a detachment fault surface on the Abel Dome, Kane oceanic core complex from Jason II on dive Kn180-2 113. (a) Section through the upper part of the fault, showing two anastomosing shear zones around a relatively coherent facoid of partially serpentinized peridotite. (b) The fault surface composed of talc-chlorite schist. Note fault striations and gentle dip.

The detachment faults at Atlantis Bank (SWIR) and Kane (MAR) have relatively thick (up to many tens of meters) zones of plastic deformation manifested as high-strain mylonitic rocks [*Dick et al.*, 2000b; *Miranda et al.*, 2003; *Hansen*, 2007; *Miranda and John*, 2010], overprinted by cataclasite and/or breccia and gouge during the down-temperature evolution of the fault system. Conversely, evidence for plastic deformation in core from Hole U1309D (Atlantis Massif) and at 15°45′N (MAR) is limited or lacking. In both cases, the detachment fault is characterized by brittle and/or semibrittle deformation, with formation of cataclasites, breccias,

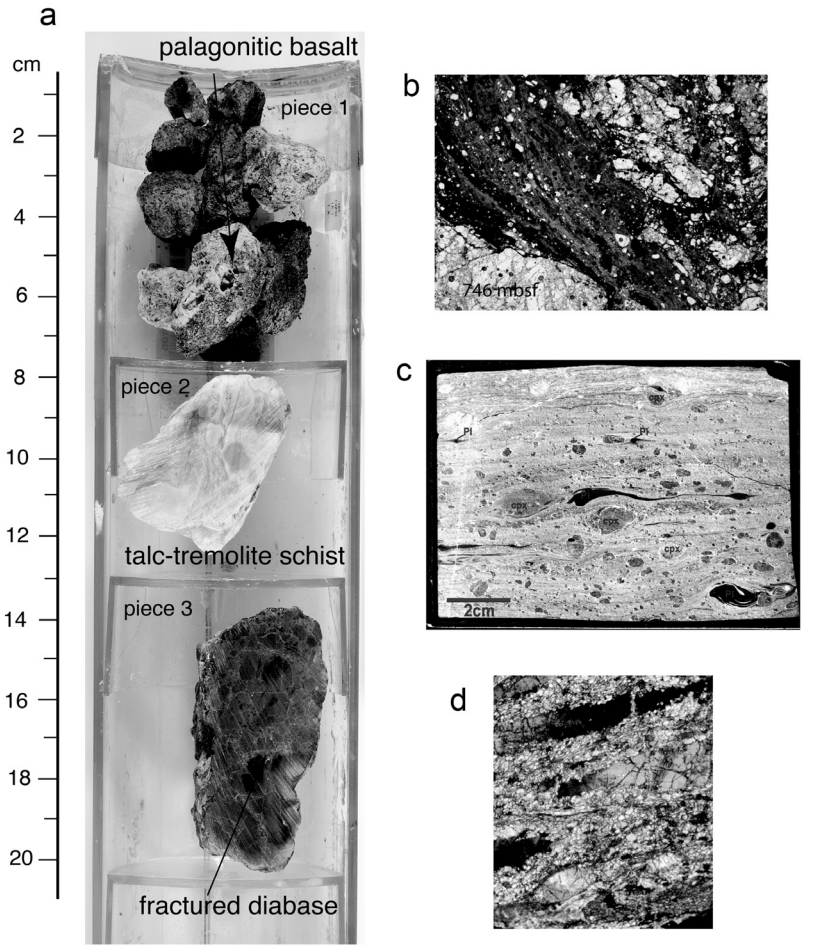

Figure 8. Macrostructural and microstructural character of oceanic detachment fault rocks. (a) Short core from the top of Atlantis Massif (Hole U1309H) includes pieces of basalt, talc-tremolite schist, and diabase cataclasite [*Blackman et al.*, 2006]. The talc-tremolite schist is similar to fault rocks recovered along portions of other oceanic detachment faults. Fracture intensity in the diabase is minor, suggesting fairly low strain but consistent with the sample being part of a process zone associated with a fault system. (b) Gabbro cataclasite from Hole U1309D (brittle fault system recovered at 746 mbsf). (c) Fe-Ti oxide bearing gabbro ultramylonite from the surface of Atlantis Bank (Shinkai dive sample 6k-460-10). (d) Peridotite mylonite from the Abel Dome, Kane core complex (sample Kn180-2 17-14; crossed polars).

and/or gouge from <1 to >10 m thick [*MacLeod et al.*, 2002; *Escartín et al.*, 2003; *Fujiwara et al.*, 2003; *Blackman et al.*, 2006; *Ildefonse et al.*, 2007]. This presence or absence of thick zones of high-strain mylonites is likely dictated by several factors including position relative to the breakaway (i.e., initial structural depth), magnitude of slip, rheology (see below), and the involvement of water during fault zone evolution.

The best constraints on fault/shear zone architecture are provided by borehole observations from three core complexes (Ocean Drilling Program (ODP)), Hole 735B [*Shipboard Scientific Party*, 1999], ODP Hole 1275D [*Kelemen et al.*, 2004], and Integrated Ocean Drilling Program (IODP) Hole U1309D [*Blackman et al.*, 2006]. Core from these holes typically shows partitioning of deformation onto more than one subhorizontal slip surface/fault zone.

In Hole 735B, fault rock recovery, logging data, and subhorizontal vertical seismic profiling reflectors indicate a 100-m-thick zone of variable plastic deformation at the seafloor, with a second roughly 90-m-thick zone of similar plastic deformation between 480 and 570 mbsf [*Cannat et al.*, 1991; *Swift et al.*, 1991; *Shipboard Scientific Party*, 1999]. Both are overprinted by semibrittle and brittle deformation. Additional data from submersible samples collected from the

surface of Atlantis Bank suggest that mylonites associated with the detachment fault system are distributed over a structural thickness up to 100 m below the fault surface exposed at the seafloor [*Matsumoto et al.*, 2002]. Semibrittle and brittle fault rocks (cataclasite, breccia, and rare gouge) are found to 120 mbsf, with the majority concentrated in the 30 m immediately below the detachment fault surface [*Dick et al.*, 2000b; *Miranda*, 2006].

Core from Hole U1309D (Atlantis Massif) suggests that deformation beneath the main detachment surface is limited (<3% in the recovered core) [*Blackman et al.*, 2006]. High-strain mylonitic shear zones are rare and typically restricted to clearly defined, dominantly granulite-grade shear zones ranging from millimeters to tens of centimeters thick. The amount of strain recorded by brittle fracture and cataclasis is also limited, except for zones of poor recovery/fault zones concentrated in the upper 150 m of Hole U1309D and in discrete intervals downhole [*Blackman et al.*, 2006]. The lack of structures indicative of significant displacement by either brittle or plastic processes severely limits the possible thickness of fault zones that would comprise a detachment system across the central dome of Atlantis Massif. Poor recovery of the upper 20 m of the footwall allows the possibility that this narrow zone accommodated very high strain along a dominantly brittle, 20-m-thick fault (Figure 8). In marked contrast, roughly 5 km south of Hole U1309D along the southern wall of Atlantis Massif, the detachment fault is characterized by an ~100-m-thick normal-sense shear zone, comprising highly deformed serpentinized peridotite and gabbro, affected by talc and/or amphibole metasomatism [*Schroeder and John*, 2004; *Boschi et al.*, 2006; *Karson et al.*, 2006]. This shear zone records high-temperature plastic deformation overprinted by lower temperature semibrittle and brittle deformation.

Fault rocks associated with oceanic detachments result from deformation of gabbro (±diabase) and peridotite dominated by the rheology of plagioclase and olivine and/or their alteration products (Figure 9). Overprinting relations indicate a down-temperature path in their formation; high-temperature strain fabrics are cut by progressively lower-temperature deformation, consistent with denudation during progressive normal faulting. To date, only a few detachment fault systems allied with oceanic core complexes have been studied in detail. However, in all cases examined, the intensity of mesoscopic deformation fabrics increases upward toward the surface exposed at the seafloor, interpreted as the oceanic detachment fault [*Dick et al.*, 1991; *MacLeod et al.*, 2002; *Escartín et al.*, 2003; *Kelemen et al.*, 2004; *Schroeder and John*, 2004; *Boschi et al.*, 2006; *Miranda*, 2006; *Karson et al.*, 2006; *Hansen*, 2007].

Gabbroic rocks drilled in Hole 735B in Atlantis Bank (SWIR) preserve microstructures indicative of an evolution from high-temperature magmatic and crystal plastic deformation, through high-temperature metamorphism and brittle-ductile deformation, to penetrative brittle deformation associated with the circulation of seawater [*Shipboard Scientific Party*, 1999]. Mylonitic fabrics are characterized by a well-developed, moderate- to gently dipping foliation, and mineral lineation. Paleomagnetic reorientation suggests this fabric originally dipped gently toward the ridge axis at ~20° degrees [*Shipboard Scientific Party*, 1999]. Lower-temperature shear-sense indicators (amphibolite and greenschist facies) are consistently top toward the ridge axis, indicating conditions of normal-sense tectonic transport. Microstructural observations and mineral thermometry from in situ submersible samples, and ODP Hole 735B samples indicate that detachment faulting initiated near magmatic conditions and continued to subgreenschist temperatures through the semibrittle and brittle regimes, as strain was localized along the exposed subhorizontal fault surface. Microstructural studies suggest that strain localization was achieved by dynamic recrystallization of plagioclase at temperatures between 950°C and 650°C [*Mehl and Hirth*, 2008], by amphibole-accommodated dissolution-precipitation creep at temperatures ~600–450°C, by chlorite-accommodated reaction softening at temperatures ~300–450°C, and by brittle fracturing and cataclasis at temperatures <300°C [*Miranda and John*, 2010].

The Kane oceanic core complex (23°N, MAR) provides additional constraints on the evolution of oceanic detachment faults with both peridotite and gabbro in the footwall [*Dick et al.*, 2008]. Fault rock samples investigated by *Hansen* [2007] indicate that the Kane detachment system records a deformation history that also initiated at temperatures >700°C and extended to below the brittle-plastic transition. The fault rocks exhibit the general down-temperature deformation history characteristic of normal faulting, from granulite and amphibolite through subgreenschist facies including brittle cataclasis. Samples collected from a high-angle fault scarp cutting the peridotite-dominated Cain Dome [*Dick et al.*, 2008] reveal an ~450-m zone of discrete ductile shear zones with peridotite mylonites, overprinted by a 200-m zone of semibrittle and brittle deformation. We note in ultramafic rocks, much of the recorded high-temperature deformation is often obscured by lower-temperature growth of serpentine minerals and may often be overlooked. These observations, taken with the strain analysis by *Hansen* [2007], imply strain localization with progressive deformation: high-temperature plastic deformation is overprinted down temperature by brittle/cataclastic fabrics. A second, contrasting section, collected from a fault scarp cutting the Adam Dome, is dominated by gabbroic rocks and shows a paucity of deformation

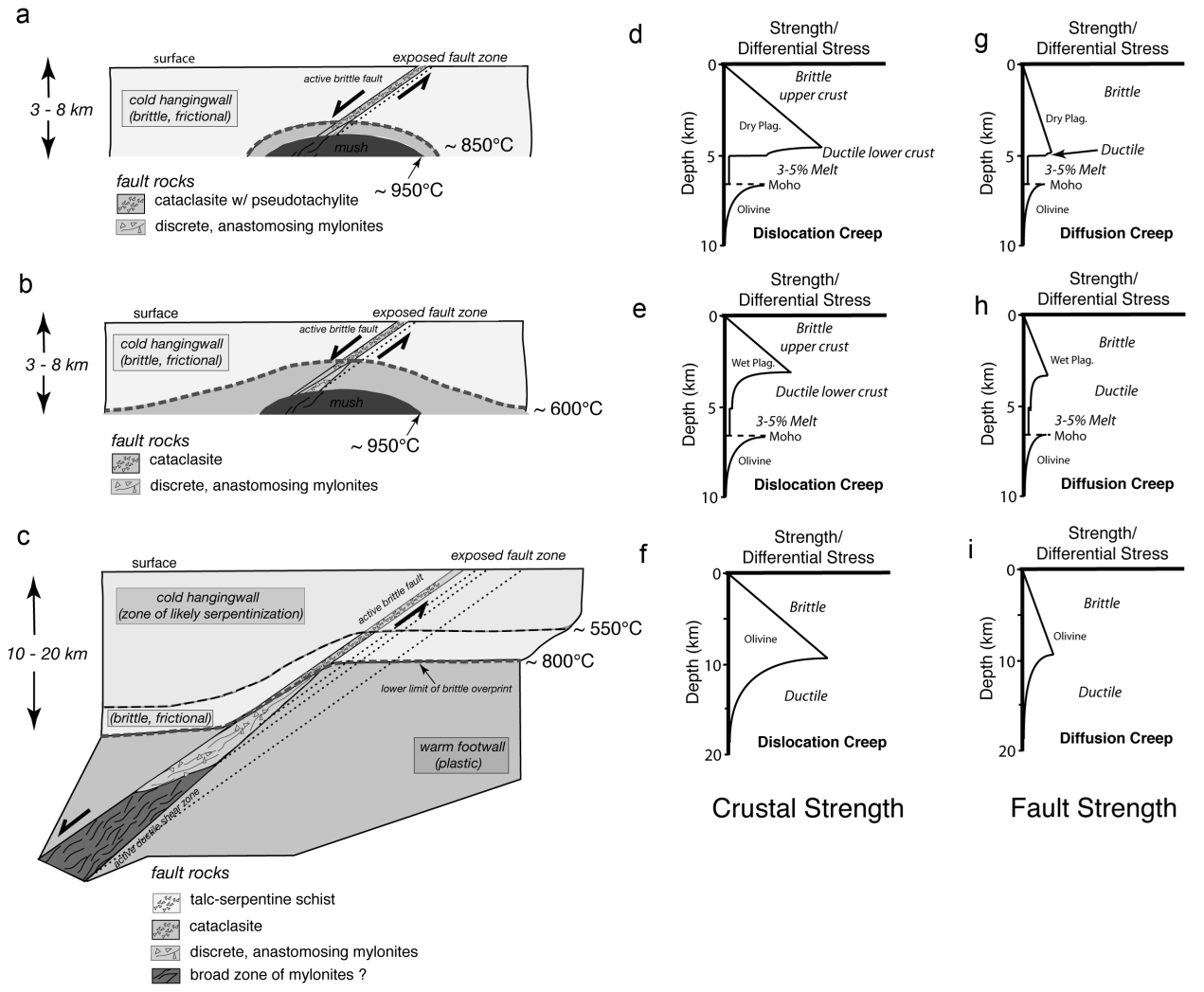

Figure 9. Schematic sections through oceanic detachment fault systems with variable rheology: (a) Detachment fault traverses crust characterized by dry plagioclase rheology and roots in a magma chamber, limited mylonites are developed in the narrow temperature interval between ~950°C and 850°C. (b) Detachment fault traverses crust characterized by wet plagioclase rheology and roots in a magma chamber. Mylonites are well developed over a temperature interval of ~350°C (between ~ 950° and 600°C). (c) Amagmatic extension. Detachment fault traverses mantle peridotite. Mylonites are developed at depths of >~10 km. Uppermost fault altered to talc-serpentine schist. Cartoon models of strength versus depth for oceanic crust and oceanic detachment faults, respectively. (d) Crust with dry plagioclase rheology. Magma mush zone creates low strength zone at the base of the crust. Weak olivine rheology due to presence of melt and advected heat. (e) Crust with wet plagioclase rheology. Magma mush zone creates low strength zone at the base of the crust. Weak olivine rheology due to presence of melt and advected heat. (f) Amagmatic extension. Crust and mantle made of olivine. (g, h, and i) Fault strength diagrams corresponding to (d), (e), and (f), respectively, assuming weakening due to reaction softening due to alteration, elevated pore pressure, and diffusion creep due to grain size reduction.

similar to that recorded by IODP Hole U1309D at Atlantis Massif. This section is within 2 km of the estimated breakaway [*Dick et al.*, 2008] and therefore accommodated slip at shallow crustal levels (≤2 km), enjoying only brittle deformation.

2.2.3. Fault zone rheology and mechanism(s) of strain localization. The presence of high-temperature mylonite associated with some oceanic detachment faults (Atlantis Bank, southern wall of Atlantis Massif, and the Kane oceanic core complex) contrast with others showing little or no evidence

for significant high-temperature plastic deformation (central dome of Atlantics Massif and 15°45′N on the MAR). We suggest this is partly a consequence of the narrow temperature window available for plastic deformation in gabbroic rocks that form oceanic crust (Figure 9). Strain will always localize in the weakest rocks; this relationship is evidenced by gabbros from ODP Hole 735B that exhibit hypersolidus/magmatic fabrics subparallel to subsolidus fabrics associated with the detachment system [*Shipboard Scientific Party*, 1999]. In slow spreading environments, the most evolved gabbros in any magma chamber are likely to be evolved amphibole bearing Fe-Ti oxide gabbros with a solidus temperature between ~850°C and 900°C [*Coogan et al.*, 2001; *Natland et al.*, 1991; *Grimes et al.*, 2008]. Therefore, if a magma chamber is present, the solidus temperature will constrain the highest temperature of mylonite/fault rock formation; above this temperature, strain can localize in partially solidified, evolved gabbro mush zones. Indeed, detachment faults at Atlantis Bank and Kane host deformed Fe-Ti oxide gabbros, suggesting strain localization in these rocks [*Dick et al.*, 2000b; *Agar and Lloyd*, 1997]. The initial distribution of the anastomosing high-temperature shear zones may therefore be a function of the distribution of evolved gabbro horizons in the crystallizing gabbro body.

The onset of semibrittle deformation can be inferred by considering upper temperature limits estimated for the hydrothermal alteration of oceanic gabbros, as hydrothermal circulation requires cracking to provide fluid pathways. *Manning et al.* [1996] suggest this occurs at ~700–750°C in gabbro from Hess Deep (East Pacific Rise), consistent with seismic estimates of the temperature of the brittle-ductile transition [*Phipps-Morgan and Chen*, 1993]. Therefore, the temperature window for the formation of plastically deformed rocks (mylonites) between the gabbro solidus and the onset of semibrittle deformation is likely only 100–200°C (Figure 9) corresponding to a time window of 50–100 ka, assuming a cooling rate on the order of 2000°C Ma^{-1} [*John et al.*, 2004]. Consequently, it may normally be very difficult to form extensive mylonite zones by detachment faulting in oceanic crust.

A second constraint for the onset of semibrittle deformation comes from rock deformation experiments. These further delimit the range of conditions viable for plastic deformation, based on both the composition of the gabbros (dominated by the mineral phases plagioclase, clinopyroxene, and olivine) and the water content of these minerals. For a fixed strain rate, the strength (viscosity) of a gabbro will increase with increasing modal pyroxene and olivine [*Mehl and Hirth*, 2008; *Burgmann and Dresen*, 2008]. Therefore, lower stresses are required for dislocation creep and the onset of mylonite formation in plagioclase-rich rocks compared to pyroxene- and olivine-rich rocks. In addition, bound water in the crystal lattice weakens all minerals allowing dislocation creep at lower stresses than dry minerals, at a given strain rate [e.g., *Rybacki and Dresen*, 2000, 2004]. *Mehl and Hirth* [2008] suggest that the differential stress required for brittle deformation on detachment faults in oceanic core complexes is between 60 and 200 MPa (over a depth range of 4–10 km), based on microstructural observations from mylonites sampled at Atlantis Bank (grain size and dominant deformation mechanism), and Goetze's criteria [*Kohlstedt et al.*, 1995].

Modeling, using diabase, mixed plagioclase and pyroxene, and wet and dry plagioclase flow laws, indicates that the stress required (at a fixed strain rate and temperature) for dislocation creep and the initiation of mylonite formation, decreases with increasing water content of the plagioclase and with decreasing pyroxene content [*Rybacki and Dresen*, 2000, 2004; *Mehl and Hirth*, 2008]. The formation of fault rocks bearing plastic deformation fabrics is therefore more likely in gabbro that host "wet" plagioclase. Water may be incorporated into the plagioclase crystal lattice during crystallization, if the magma chamber contains water, perhaps due to digestion of hydrothermally altered earlier-formed gabbros [*Coogan et al.*, 2001]. The presence of magmatic amphibole with elevated chlorine concentrations in some gabbros indicates that gabbroic melts can be contaminated with seawater [*Maeda*, 2002]. Calculations using flow laws from *Rybacki and Dresen* [2004] and *Dimanov and Dresen* [2005], suggest that at reasonable strain rates (10^{-12} s^{-1}), dry polyphase gabbro may require stresses of 50–100 MPa to undergo plastic deformation at temperatures of ~900°C. These stresses are similar to estimates using Goetze's criteria, and consequently, gabbroic rocks may transition directly from magmatic crystallization to brittle deformation, without any significant plastic deformation. Conversely at similar strain rates, wet gabbro may undergo crystal plastic deformation at 1–10 MPa and, therefore, traverse the plastic-brittle transition at lower temperatures (500–600°C), undergoing crystal plastic deformation over a 300°C temperature window from solidus temperatures of 900°C.

We hypothesize that the presence or absence of significant zones of crystal plastic deformation associated with oceanic detachment fault systems, in part, reflects the composition and therefore rheology of the gabbroic rocks the fault traverses. Figure 9 shows models to explain the variable nature of detachment faults cutting oceanic lithosphere, highlighting the relatively restricted range of conditions for mylonite formation in gabbroic crust. In addition, the figure shows schematic strength-depth diagrams illustrating the rheological behavior of wet and dry ocean crust, and emphasizes that thick mylonite zones are best developed in wet oceanic crust. If gabbroic crust is not present, thick

peridotite mylonites may develop at depth if the detachment fault roots into magma-absent mantle peridotite (Figure 9c). Recovery of fresh peridotite mylonite from the Kane core complex [*Hansen*, 2007], as well as from the south wall of Atlantis Massif [*Schroeder and John*, 2004], supports this model.

The low-temperature rheology of the fault zone is governed by the temporal history of cracking and hydrothermal circulation leading to the formation of the talc ± chlorite ± tremolite schists and rare clay gouge recovered from oceanic detachment faults. These schists and gouges likely lower the coefficient of friction to allow slip and, therefore, the longevity of the detachment faults once initiated. Serpentinization of olivine in mafic and/or ultramafic rocks can lead to fault weakness, strain localization, and slip under low resolved shear stress [*Francis*, 1981; *Cannat*, 1993; *Escartin et al.*, 1997]. Fracturing, fluid flow, and localization of serpentinization in peridotite will allow deformation to concentrate in a fault zone.

2.2.4. Detachment fault depth and dip. The observation that the domes of the core complexes are bathymetrically smooth and often extend for 10–30 km downdip suggests that they represent the footwalls to a single large normal fault, whose active portions may extend several kilometers below the seafloor. The subsurface geometry of oceanic detachment faults has been subject of much debate, with some authors suggesting relatively gently dipping (10–20°) planar faults, which root in either the dike-gabbro transition or an alteration front [*Escartín et al.*, 2003], whereas others [*Lavier et al.*, 1999; *Buck et al.*, 2005] have suggested that the faults initially dip steeply (~50–60° at depths of 3–7 km) and "roll over" to form the core complex. We present observations to suggest that the latter model is likely correct.

Exposures of fault surfaces exposed at the seafloor associated with oceanic core complexes have dips of 5° to 15° at their terminations, suggesting that the faults had initial dips of at least this magnitude. Some core complexes (Kane at 23°N and at 13°N on the MAR) have recognizable upturned "breakaway ridges" formed by the flexural response of thin lithosphere to large-magnitude slip [*Hansen*, 2007; *Smith et al.*, 2008]. The outward facing slope of these ridges was the original subhorizontal seafloor before fault slip, whereas the inward facing slope is the detachment fault surface. The angle between the outward and inward facing slopes therefore provides an estimate of the initial detachment fault dip. *Smith et al.* [2008] and *Hansen* [2007] use this method to suggest initial dips at the Kane and 13°N core complexes >45°. Paleomagnetic studies at 15°N on the MAR [*Garces and Gee*, 2007], at Atlantis Bank [*Shipboard Scientific Party*, 1999; *Worm*, 2001], and at Atlantis Massif [*Morris et al.*, 2009] suggest footwall rotations of 50°–80°, 20°, and 35°, respectively, below the temperature for acquisition of magnetization (Curie temperature ~500°C ± 50°C). These rotations are minimum values, as the faults may well have been active above the Curie temperature and root in higher temperature rocks [*Schroeder and John*, 2004; *Hansen*, 2007; *Mehl and Hirth*, 2008]. Microearthquake hypocenters recorded beneath the trans-Atlantic geotraverse (TAG) hydrothermal field at 26°N on the MAR dip at 70° and define an arcuate, domal surface interpreted as the subsurface expression of a detachment fault [*deMartin et al.*, 2007]. These observations, together with deformation temperature estimates for fault rocks of 700–800°C, support a "rolling hinge" model for rapid flexural rotation of steep normal faults with an elastic thickness Te ~1 km [*Lavier et al.*, 1999]. *Smith et al.* [2008] conclude a similar elastic thickness for the breakaway regions of oceanic detachment faults, based on modeling bathymetry. The low Te's partially reflect the intense deformation recorded by the footwall, with brittle shear zones extending to hundreds of meters below the detachment fault [*Shipboard Scientific Party*, 1999; *Kelemen et al.*, 2004; *Blackman et al.*, 2006]. The depth of fault penetration is likely a function of geothermal gradient and the nature of the rocks at the ridge axis. If magma chambers are present, the faults likely root into the magma chamber; if magma is not present, the faults may root to depths of 5–10 km, corresponding to the depth of seismicity on some regions of slow spreading ridges [*Toomey et al.*, 1988; *Kong et al.*, 1992; *Canales et al.*, 2005; *deMartin et al.*, 2007]. Below these depths, the faults most probably transition through localized zones of ductile deformation, into zones of broadly distributed plastic deformation within the mantle.

Ildefonse et al. [2007] have hypothesized that large gabbroic intrusions may be required to localize strain and develop oceanic detachment faults owing to the rheological differences between gabbro and serpentinized peridotite [*Escartin et al.*, 1997]. In these models, oceanic detachment faults may consist of thin sheaths of deformed talc/serpentinized peridotite surrounding low-strain gabbro cores. The existence of high-strain peridotite and gabbro mylonite in the detachment faults on the south wall of Atlantis Massif [*Schroeder and John*, 2004], at Kane [*Hansen*, 2007; *Dick et al.*, 2008], and at Atlantis Bank [*Miranda*, 2006; *Mehl and Hirth*, 2008] suggest that detachment faults can, however, initiate at depth away from the influence of hydrothermal circulation. Further, the existence of a detachment fault within peridotite at the Kane core complex suggests that although strain may localize adjacent to a gabbro body when such a body is in a fortuitous orientation, large gabbro bodies are not required to focus strain and nucleate detachment faults.

2.2.5. Oceanic detachment faults are not conservative. If detachment faults in oceanic lithosphere initiate as high-angle normal faults cutting through ocean crust, then the footwall adjacent to the breakaway should expose a section through that crust. Assuming an initial dip of ~50° and an initial crustal thickness of 6 km implies that the first 8 km of footwall (measured from the breakaway) likely exposes a complete crustal section. In many cases, the exposed footwall of an oceanic core complex is much greater than 10 km and commonly up to 30 km in the slip direction (with Godzilla Megamullion up to 125 km long). The exposed footwall is therefore often much greater than the initial thickness (~5–7 km) of ocean crust and much greater than the seismically determined length of the initial fault (up to 10 km). In effect, the footwall is much longer than the hanging wall, resulting from continuous fault slip allowing new footwall to be generated from the mantle or by crystallization of new gabbroic crust in any magma chamber in which the fault roots. Consequently, detachment faults associated with oceanic core complexes are nonconservative; they cannot be structurally restored and likely are formed by a continuous casting process (Figure 10) [*Spencer*, 1999; *John and Cheadle*, 2005]. *Dick et al.* [2000a] has termed detachment faults that are nonconservative and which root in magma chambers, plutonic growth faults.

2.2.6. Strain rates, slip rates, and ridge migration. Detailed microstructural studies of rocks from the Kane complex [*Hansen*, 2007], and at Atlantis Bank, SWIR [*Miranda*, 2006], both confirm localization of strain during the evolution of the detachment fault zones, from thick ductile shear zones into narrower zones of semibrittle deformation, leading to an increased strain rate with time. *Hansen* [2007] and *Mehl and Hirth* [2008] report strain rates of 10^{-12}–10^{-14} s^{-1} for granulite-grade ductile shear zones in gabbro and peridotite from the Kane core complex, and for granulite-grade deformation in gabbro from Atlantis Massif. *Miranda* [2006] and *Hansen* [2007] both report faster strain rates of 10^{-10}–10^{-12} s^{-1} for lower-temperature, amphibolite-grade mylonitic gabbros from Atlantis Massif and the Kane area. This increase in strain rate is consistent with strain localization from high-temperature shear zones up to 100 m thick, to lower temperature shear zones a few meters thick.

Schroeder and John [2004] showed that detachment faults represent the plate boundary, and accommodate a significant portion of the plate spreading. Various authors [*Schultz et al.*, 1988; *Searle et al.*, 2003; *Okino et al.*, 2004; *Williams*, 2007; *Baines et al.*, 2008; *Grimes et al.*, 2008] have shown, using both magnetic and thermochronometric methods, that core complexes are not only structurally asymmetric, but also form during asymmetric plate spreading. Estimates for time-averaged slip rates on oceanic detachment faults during core complex formation range from ~14 km Ma^{-1} at Atlantis Bank [*Baines et al.*, 2008], up to 24 km Ma^{-1} at Atlantis Massif [*Grimes et al.*, 2008], to at least 38 km Ma^{-1} for the

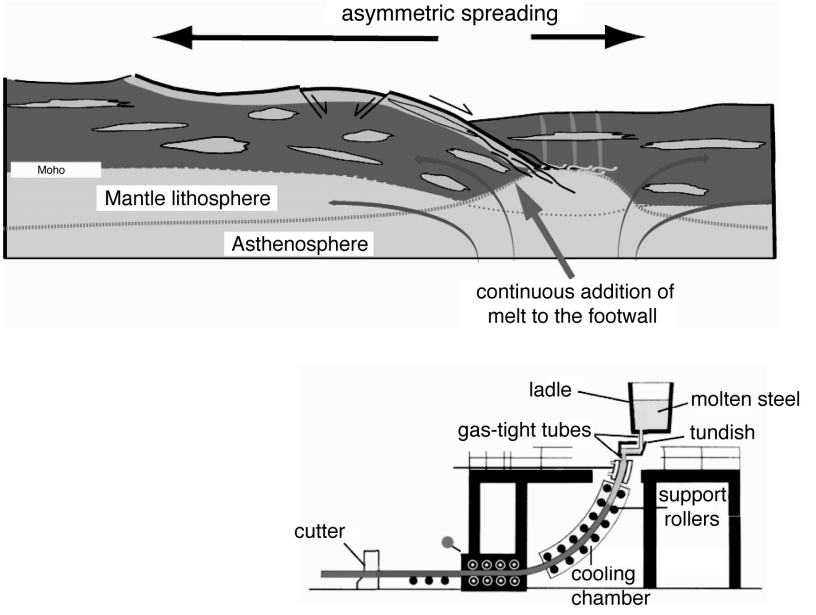

Figure 10. Cartoon of "continuous casting" for the development of oceanic detachment faults (cross-section modified from *Escartín et al.* [2003]).

Godzilla Megamullion [*Ohara et al.*, 2001]. Consequently, core complexes apparently form during periods of 60–100% asymmetric spreading. The best-documented example of this is Atlantis Bank [*Baines et al.*, 2008], where not only does the local spreading rate increase to 80% asymmetry of the full rate, but this increase in rate is also confined to the ridge segment in which Atlantis Bank occurs (Figure 11). As a consequence, offset on the adjacent small-offset transform fault decreases from 20 to 0 km, and most importantly, the ridge axis migrates relative to the adjacent segment. If core complexes are formed during local periods of asymmetric spreading, an essential consequence of this is ridge axis migration away from the core complex with respect to adjacent ridge segments. We hypothesize that the detachment fault therefore must either flatten with time or "jump" to a location closer to the ridge axis. We suggest that the flattening of a detachment fault through time is testable by determining the orientation of the magnetic vector in samples collected along a flow line over the domal fault exposure.

Figure 12 shows conceptual cartoons after *Baines et al.* [2008], demonstrating how plate separation and extension may be accommodated with depth. In the amagmatic case (A), plate separation is dominated by detachment faulting to depths of 10–12 km and by ductile corner flow in the mantle below. A minor component of plate separation may be accommodated by diking and limited magma intrusion below the dikes, and by late, brittle high-angle faulting. This illustrates the case for magma-starved regions such as 15°N on the MAR. Figure 12b shows the case where a detachment fault roots into a zone of magmatic accretion. In this case, the detachment fault accommodates plate separation to ~4 km depth, with magmatic accretion accommodating plate separation at greater depths to the Moho, and mantle separation is accommodated by corner flow. Although these diagrams are conceptual, they highlight the possibility that both detachment faulting and magmatic accretion together accommodate plate separation. This latter cartoon illustrates the case for an "Atlantis Bank" type oceanic core complex.

2.2.7. Hydrothermal alteration and evidence for fluid flow. In contrast to the very limited studies of hydrothermal alteration allied with continental detachment fault systems, equivalent studies in the oceans are numerous. Many authors have suggested a direct link between oceanic detachments faults and hydrothermal vent fields of variable temperature, including TAG at 26°N on the MAR [*Tivey et al.*, 2003; *deMartin et al.*, 2007; *McCaig et al.*, 2007, this volume], Rainbow at 36°N on the MAR [*Charlou et al.*, 2002; *Gràcia et al.*, 2000; *McCaig et al.*, 2007], and Lost City at 30°N on the MAR [*Kelley et al.*, 2001; *Schroeder et al.*, 2002; *Boschi et al.*, 2006; *McCaig et al.*, 2007]. As in continental settings, hydrothermal circulation requires cracking and the availability of fluids. Brittle fracture associated with detachment fault slip provides the pathways for fluid circulation and alteration. Three styles of alteration have been documented associated with oceanic detachment fault systems and fluid type: (1) hanging wall-derived fluids (basalt interaction with seawater), (2) fluids derived near the breakaway (likely similar to hanging wall fluids), and (3) fluids associated with metamorphic reactions and magmatism in the footwall (likely dominated by serpentinization reactions). Additionally, fluid-rock interaction and igneous activity can be coeval with detachment faulting [*MacLeod et al.*, 2002; *Escartín et al.*, 2003; *Blackman et al.*, 2006].

The two deep boreholes into oceanic core complexes provide the most complete evidence of hydrothermal alteration and fluid flow along and below detachment faults. In both cases (Atlantis Massif, MAR-IODP Hole U1309D, and Atlantis Bank, SWIR-ODP Hole 735B), the recovered sections are moderately altered at conditions ranging from magmatic to zeolite facies [*Shipboard Scientific Party*, 1999; *Blackman et al.*, 2006]. While there is a spectrum of metamorphic facies in both holes, an overall decrease in total alteration and a change in style of alteration occur with depth.

Gabbroic rocks recovered from Hole 735B record a complex metamorphic history [*Dick et al.*, 2000a, 2000b]. The highest temperature alteration is shown by the presence of secondary amphibole at temperatures up to 700°C closely related to ductile deformation and synkinematic cracking [*Stakes et al.*, 1991; *Vanko and Stakes*, 1991; *Bach et al.*, 2001; *Miranda*, 2006]. Both the main detachment (exposed at the seafloor) and the structurally deeper low-angle fault preserved at a depth of ~500 m in Hole 735B are marked by moderate-to-high temperature amphibole schist and gneiss, characterized by well-developed protomylonite and mylonitic textures, in turn, cut by orthogonal monomineralic amphibole veins, formed at essentially the brittle-plastic transition [*Agar*, 1994; *Shipboard Scientific Party*, 1999]. The abundance of secondary amphibole in the zones of plastic deformation suggests they represent major conduits for hydrothermal fluids. Detailed petrologic studies of rocks collected from both ODP Hole 735B and IODP Hole U1309D also show evidence for "hydromagmatic" growth of trace minerals (e.g., epidote) implying high-T fracture and entrainment of seawater in late-stage residual melts to depths of >635 m below seafloor [*Maeda*, 2002].

Alteration and metamorphic vein intensity decrease markedly downward in both deep boreholes that penetrate the footwalls of oceanic core complexes. In Hole 735B, hydrothermal vein systems form 1–2.4% of the core and comprise mainly plagioclase, amphibole, diopside, carbonate, variable

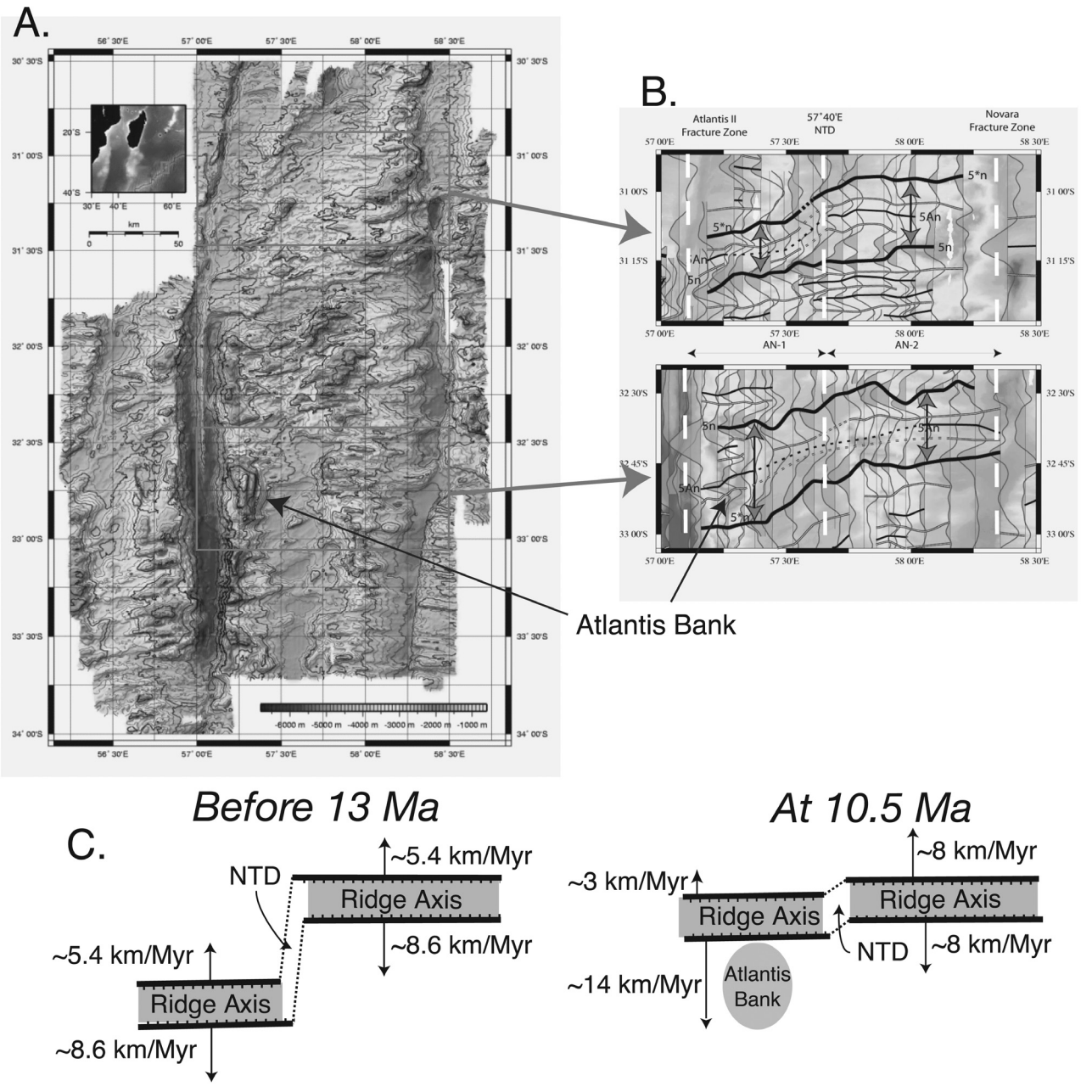

Figure 11. Asymmetry of plate spreading during formation of Atlantis Bank, SWIR. (a) SeaBeam bathymetry showing the location of Atlantis Bank with respect to the Southwest Indian Ridge. Inset shows the location of the map relative to Madagascar. Outlined boxes show the areas in Figure 11b. (b) Conjugate SeaBeam bathymetry maps overlain with crustal magnetization anomalies from *Baines et al.* [2007]. Normal polarity magnetic anomaly picks shown by bold lines; reverse polarity picks by open lines. White dashed lines denote segment boundaries. Arrows highlight the distance between the 5n and 5*n anomalies, which indicate increased asymmetric spreading in the segment-containing Atlantis Bank compared to the adjacent segment. After formation of Atlantis Bank, magnetic anomaly 5n trends approximately E-W, indicating, that asymmetric spreading at Atlantis Bank led to ridge migration and reduced offset on the intervening nontransform discontinuity. (c) Cartoon to show reduction of the nontransform discontinuity (NTD) as a consequence of ridge migration related to the formation of Atlantis Bank.

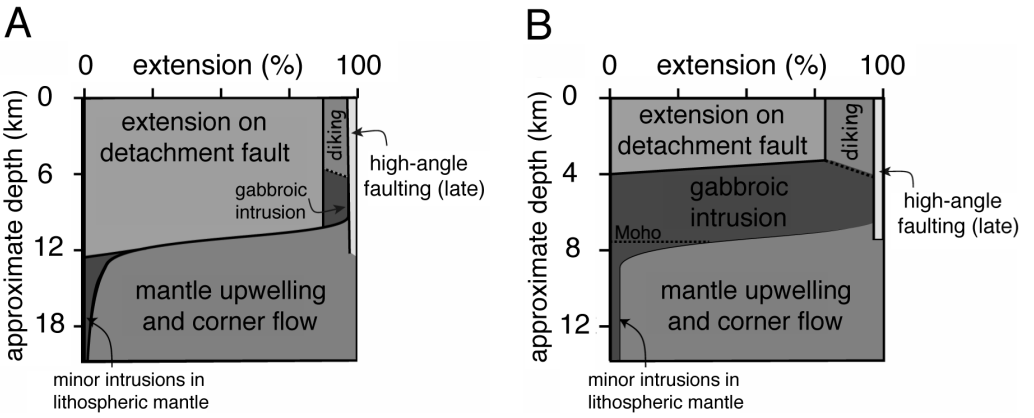

Figure 12. Conceptual extension versus depth diagrams after *Baines et al.* [2008], showing accommodation of plate separation and asymmetric detachment faulting with depth. (a) Magma-starved detachment faulting. Most plate separation is accommodated by detachment faulting to 10–12 km and by ductile corner flow in the mantle below that. A minor component of plate separation is accommodated by magmatic diking in the hanging wall plate and limited magma intrusion below the dikes, and by late, brittle high-angle faulting. (b) Magmatic case. Detachment faulting accommodates plate separation to 4 km, and magmatic accretion accommodates plate separation from 4 km down to the Moho, below which separation is accommodated by mantle corner flow. A minor component of plate separation is accommodated by magmatic diking in the hanging wall, limited magma intrusion below the dikes, and by late brittle high-angle faulting.

phyllosilicates (smectite, chlorite, talc, and serpentine). Their occurrence is interpreted to result from seawater percolation into open fractures and faults to depths of 700–1000 m below the detachment fault, at different temperatures during cooling of the footwall [*Bach et al.*, 2001; *Robinson et al*., 2002]. The upper 380 m of Hole U1309D shows an alteration profile characteristic of pervasive static infiltration of seawater with decreasing temperature; at greater depths, alteration is generally restricted to halos adjacent to veins, fractures, and igneous contacts.

Based on the distribution of metamorphic mineral assemblages in these two holes (735B, SWIR and U1309D, MAR), there is good evidence for focused or heterogeneously distributed fluid flow, concentrated along fault zones/fracture systems [*Shipboard Scientific Party*, 1999; *Blackman et al.*, 2006]. This relation implies limited heat removed by pervasive fluid flow. Local zones of high fracture intensity and brittle deformation are commonly mineralized by late, low-temperature infiltration of seawater and assemblages including smectite, chlorite-smectite, carbonate, zeolite, analcite, and phrenite, even at significant depths [*Bach et al.*, 2001]. O-isotope data from ODP Hole 735B indicate significant seawater interaction in the upper 200 m of the core decreasing downward and dying out below ~800 mbsf [*Stakes et al.*, 1991; *Gao et al.*, 2006], consistent with the distribution of amphibole veins [*Shipboard Scientific Party*, 1999; *Bach et al.*, 2001]. *deMartin et al.* [2007] suggest that earthquakes penetrate to depths of 6.5–7 km depth below the MAR in the TAG region, likely associated with detachment faulting. This evidence for cracking/brittle failure implies fluid flow to significant depths in oceanic core complexes. With high-angle faulting penetrating to depths of 6–8 km, steeply dipping isotherms adjacent to the faults may lead to focused flow [see *Morton and Sleep*, 1985], which in turn might set up an asymmetric thermal structure in slow spreading oceanic lithosphere associated with core complex formation. Based on cooling rate estimates of gabbro recovered from ODP Hole 735B and around Atlantis Bank using geochronometry and thermochronometry [*John et al.*, 2004; *Schwartz et al.*, 2009], we suggest that cooling of the rock body (and attendant cracking) at temperatures below ~700°C took place in <300 ka (within ~4 km of the ridge axis).

Metasomatic (and deformation enhanced) alteration of gabbro and peridotite to talc- and/or amphibole-bearing assemblages is a key aspect of the detachment fault system exposed on the southern wall of Atlantis Massif [*Schroeder and John*, 2004; *Boschi et al.*, 2006; *Karson et al.*, 2006], at Atlantis Bank [*Miranda*, 2006], and at 15°N on the MAR [*MacLeod et al.*, 2002; *Escartín et al.*, 2003]. *MacLeod et al.* [2002] show evidence for a spectrum of temperatures from amphibolite to subgreenschist facies in gabbroic rocks associated with fault rocks developed at 15°45′ on the MAR.

There the surface of the massif is interpreted as a fault zone composed of talc-tremolite-chlorite schists, metamorphosed at greenschist grade, with a footwall composed of serpentinized peridotite intruded by gabbro [*Escartín et al.*, 2003]. Similar talc-tremolite schists are reported from detachment faults elsewhere in the Atlantic including 30°N [*Schroeder and John*, 2004; *Blackman et al.*, 2006; *Boschi et al.*, 2006; *Karson et al.*, 2006], and 23°N [*Hansen*, 2007; *Dick et al.*, 2008], and at Atlantis Bank, along the SWIR [*Arai et al.*, 2000]. Fault rock textures indicate replacement of harzburgite by talc + tremolite, and basalt by chlorite ± tremolite and/or actinolite [*Escartín et al.*, 2003]. These coupled reactions involving the mass transfer of Ca and Si occur wherever fluids exchange between mafic and ultramafic rocks under greenschist facies conditions [*McCaig et al.*, 2007]. Alteration of both mafic and ultramafic rock types, to form schists, involve significant chemical mass transfer and, at least locally, deformation. Fluid-rock interaction and igneous activity are thought to have been coeval [*MacLeod et al.*, 2002; *Escartín et al.*, 2003; *Blackman et al.*, 2006].

Using Sr- and O-isotope and rare earth element (REE) chemical data, *McCaig et al.* [2007] show evidence for high fluid fluxes along oceanic detachment faults. The metasomatic fault rocks formed part of the reactive pathway for a hanging-wall black smoker system similar in composition to the ultramafic-hosted Rainbow vent field, with fluids characterized by low pH and high abundances of Fe, Mn, Ca, Y, and REEs compared to mafic-hosted vent systems [*Douville et al.*, 2002]. They conclude that intense metasomatic and isotopic alteration in the fault rocks indicate that large fluid volumes were focused along the detachment under greenschist-grade conditions. There is increasing physical evidence for a link between vent fields on slow and ultraslow spreading ridges and low-angle detachment faults [*Tivey et al.*, 2003; *German and Lin*, 2004; *deMartin et al.*, 2007]. Hydrothermal vents controlled by such low-angle faults may be located significantly off axis (kilometers away from the main volcanic zone or magma chamber) and could be unusually long-lived [cf. *German and Lin*, 2004].

In summary, cracking, hydrothermal fluid flow, and alteration, with attendant metasomatic reactions typically accompany detachment faulting at oceanic core complexes. Hydrothermal fluids clearly play an important role in faulting and strain localization, whether the core complex footwall comprises peridotite or gabbro [*Escartín et al.*, 2003; *Schroeder and John*, 2004; *Miranda et al.*, 2003; *McCaig et al.*, 2007]. Although there is little evidence for an early, high-temperature influx of water during initiation of oceanic detachments, significant evidence exists for late involvement of fluids in altering (and likely reducing friction/weakening) the fault zone to produce talc, chlorite, and/or serpentine [*Escartín et al.*, 2003; *McCaig et al.*, 2007], and other "weak" minerals (smectite-bearing gouge, etc). The abrupt decrease in strength of peridotite at even small degrees of serpentinization (<15%) [*Escartín et al.*, 1997] produces a profound rheological contrast between a serpentine-free lithosphere, and a weaker, slightly serpentinized lithosphere. Penetration of fluids along permeable pathways is likely to induce marked weakening upon formation of serpentine and a range of other secondary minerals (e.g., talc, chlorite), localizing strain very efficiently onto large, discrete shear zones. Together, these processes may promote aseismic slip once the fault is initiated, seawater has accessed the damage zone, and deformation-enhanced mineral transformation has begun.

3. DISCUSSION

Two end-member types of large-offset normal faulting are attributed to plate spreading and extension along magma-limited mid-ocean ridges. In magma starved settings, mantle peridotite is denuded to the seafloor along moderate to large offset (~−5–10 km) normal faults. These faults rollover to form "smooth" ridges parallel to rift valley seen at the eastern SWIR [*Cannat et al.*, 2006], and at 15°N on the MAR [*Schroeder et al.*, 2007], and may account for >60% of the seafloor locally. At ridges with a low-moderate magma supply, oceanic core complexes sensu stricto form [*Tucholke et al.*, 2008; *Smith et al.*, 2008]. These domal features unroof gabbro and peridotite, may locally comprise from 3% to 60% of the seafloor and are bound by detachment faults with large offsets (10–125 km). Detachment faults associated with these core complexes likely originated as high-angle faults that rolled over as a flexural response to the large magnitude extension.

Strain rates and thermal gradients associated with mid-ocean ridges, together with the rheological properties of the ocean lithosphere, limit development of thick mylonitic shear zones associated with plate spreading. The brittle-plastic transition for "dry" gabbro is only ~100°C below the evolved gabbro solidus. Therefore, in many cases, fault-related deformation might transition from the magmatic regime directly to the semibrittle domain. We suggest that mylonitic shear zones are more likely to form if footwall gabbro minerals are "wet"; that is, they contain water within their crystal lattice. However, high temperature mylonite shear zones are a necessary component of plate spreading if a ridge segment is amagmatic and the fault roots into mantle peridotite.

The significant variation in footwall rock type and structural style between individual oceanic core complexes (some hosted by significant evolved gabbro in the footwall-Atlantis Bank, whereas others with more primitive gabbro and/or peridotite-Atlantis Massif), are likely a function of magma

supply, thermal structure, and spreading rate. Variations in these parameters can lead to differences in the depth of interaction between a detachment fault and magma supply. Cold, magma-starved ridges likely support deeply rooted (up to 10 km), short-lived detachment faults (5–10 km slip), whereas "warm" ridges with reasonable magma supply are likely to have shallow-rooted (4–6 km), large offset (10–30 km) detachment faults.

To encompass the range of structural characteristics and temporal history of oceanic detachment fault systems, we envision a model for their development in which the footwall is continuously accreted during fault slip: the continuous casting model (Figure 10). If magmatism dominates, the exposed footwall will comprise a large tract of midcrustal to lower crustal gabbro; if magmatism is reduced or episodic, the footwall may comprise a mixed suite of peridotite and gabbro, with screens of peridotite separating individual pulses of gabbro. In both cases, a relatively constant level of lithosphere, equating to the depth of the root zone is exposed; shallow-level gabbro-peridotite contacts do not equate to a conventional crust-mantle boundary.

4. CONCLUSIONS

Oceanic core complexes share many similarities with those on the continents; both are characterized by corrugated, domal topography; exposures of the doubly plunging fault surfaces vary up to tens of kilometers in the downdip (ridge-normal) direction, with dips ≤20°. The fault systems comprise a network of anastomosing fault/shear zones, with associated fault rocks (mylonite-cataclasite and gouge) from 1 to >200 m thick, typically exhibiting a progressive down-temperature continuum in deformation. Both form at strain rates ~10^{-12}–10^{-14} s^{-1} and are structurally asymmetric. Despite these similarities, the two systems exhibit significant differences in their evolution:

1. Oceanic detachment faults form in thinner lithosphere and are consequently associated with steeper thermal gradients than their continental counterparts.

2. Oceanic detachment faults appear to have an intimate association with magmatic accretion, gabbro bodies form an integral part of the footwall. Very reduced magmatism apparently leads to formation of fault-bound ridges rather than core complexes. Magmatism is less commonly associated with detachment faults in continental settings.

3. Differences in the composition of oceanic and continental crust fundamentally control the rheology of the detachment faults in both settings. Oceanic detachment fault systems are controlled by olivine-/serpentine-/talc- and/or plagioclase-dominated rheology, whereas continental detachment faults are controlled by a quartz and feldspar rheology. Thick zones of plastic deformation (mylonite) are likely to be absent or limited in oceanic detachment faults.

4. Fault rocks associated with the evolution of oceanic detachment faults follow a down-temperature path from magmatic to very low-temperature deformation; variations in thickness and the intensity of ductile and/or brittle deformation depend on the magnitude of slip and proximity to the fault breakaway. In continental settings, both syntectonic magmatic fabrics and high-temperature fault rocks are less common, likely due to a lower geothermal gradient.

5. Hydrothermal circulation and the consequent alteration is much more pronounced in oceanic detachment faults, and may dominate the low-temperature rheology of these fault systems.

6. Oceanic detachment faults are "new" faults; they do not interact with or reactivate preexisting anisotropies/weaknesses or older faults.

7. Oceanic detachment faults appear to be rolling-hinge-type normal faults. Paleomagnetic data from the footwalls of several oceanic detachment faults suggest rotations of 20°–80° since acquisition of remnant magnetization (passed below the Curie temperature of ~500°C ± 50°C, and their magnetic signature established), consistent with models for flexural rotation. In contrast, many continental detachment faults were demonstrably initiated at a low angle (dips ≤20°).

8. Detachment faults cutting oceanic lithosphere are clearly nonconservative; in many cases, the footwall comprises gabbro emplaced as spreading was accommodated at the ridge axis. Like continental detachments, the denuded footwall can extend for tens to over one hundred kilometers in the slip direction; hanging wall blocks above oceanic detachments may be no more than 1 km across in the dip direction.

9. Beneath continental core complexes, lower crustal flow may be common and serve to maintain crustal thickness despite significant extension. The rheology of plagioclase implies that lower crustal flow beneath oceanic core complexes is limited, and any flow is restricted to regions around magma chambers.

It is becoming increasingly apparent that at slow and ultraslow spreading ridges, the heterogeneous supply of magma requires normal faulting to accommodate a significant proportion of plate separation. These faults have apparent large offsets (>5 km); given the small elastic thickness of the plates at the ridge axis, the faults roll over to produce the low-angle fault surfaces that are readily recognized in the bathymetry [*Buck et al.*, 2005]. Consequently, such features are a fundamental component of mid-ocean ridge processes and formation of ocean lithosphere in these settings.

Acknowledgments. The evolution of ideas presented in this chapter come from many discussions with numerous people including Gary Axen, A. Graham Baines, Donna Blackman, Roger Buck,

Erin Campbell-Stone, Greg Davis, Henry Dick, Dave Foster, Phil Gans, Jeff Gee, Craig Grimes, Greg Hirth, Keith Howard, Elizabeth Miller, Julia Miller, Elena Miranda, Hans Schouten, Tim Schroeder, Rick Sibson, Jon Spencer, and Brian Wernicke. We thank Baines and Schroeder for providing inspiration for Figures 6, 11, and 12. We admit that merging ideas and observations from both marine and continental perspectives is difficult, so that reviews by Jon Spencer and Rob Reeves-Sohn helped clarify the text. Partial funding for this work was provided by NSF OCE grants 0352054 and 0752558 to Cheadle and John, OCE grant 0550456 to John, and EAR grant 9405175 to John.

REFERENCES

Abers, G. A. (2001), Evidence for seismogenic normal faults at shallow depths in continental rifts, in *Non-volcanic Rifting of Continental Margins*, *Geol. Soc. Spec. Publ.*, vol. 187, edited by R. C. L. Wilson et al., pp. 305–318.

Agar, S. M. (1994), Rheological evolution of the ocean crust: A microstructural view, *J. Geophys. Res.*, *99*, 3175–3200.

Agar, S. M., and G. E. Lloyd (1997), Deformation of Fe-Ti oxides in gabbroic shear zones from the MARK area, *Proc. Ocean Drill. Program Sci. Results*, *153*, 123–135.

Altherr, R., F. Henjes-Kunst, A. Matthews, H. Friedrichsen, and B. Tauber Hansen (1988), O-Sr isotopic variations in Miocene granitoids from the Aegean: Evidence for an origin by combined assimilation and fractional crystallization, *Contrib. Mineral. Petrol*., *100*, 528–541.

Anderson, E. M. (1942), *The Dynamics of Faulting and Dyke Formation with Application to Britain*, 191 pp., Oliver and Boyd, Edinburgh.

Arai, S., et al. (2000), Investigation of Atlantis Bank and the SW Indian Ridge from 57°E to 62°E, Mode 2000 preliminary report, JAMSTEC Deep Sea Res., Yokosuka, Japan.

Armstrong, R. L. (1972), Low-angle (denudation) faults, hinterland of the Sevier Orogenic Belt, Eastern Nevada and Western Utah, *Geol. Soc. Am. Bull.*, *83*, 1729–1754.

Armstrong, R. L. (1982), Cordilleran metamorphic core complexes —From Arizona to Southern Canada, *Annu. Rev. Earth Planet. Sci.*, *10*, 129–154, doi:10.1146/annurev.ea.10.050182.001021.

Axen, G. J. (2004), Mechanics of low-angle normal faults, in *Rheology and Deformation in the Lithosphere at Continental Margins*, edited by G. Karner et al., pp. 46–91, Columbia Univ. Press, New York.

Axen, G. J., and J. M. Bartley (1997), Field test of rolling hinges: Existence, mechanical types, and implications for extensional tectonics, *J. Geophys. Res.*, *102*, 20,515–20,537.

Axen, G. J., and J. Selverstone (1994), Stress-state and fluid-pressure level along the Whipple detachment fault, California, *Geology*, *22*, 835–838.

Bach, W., J. C. Alt, Y. L. Niu, S. E. Humphris, J. Erzinger, and H. J. B. Dick (2001), The geochemical consequences of late-stage low-grade alteration of lower oceanic crust at the SW Indian Ridge: Results from ODP Hole 735B (Leg 176), *Geochim. Cosmochim. Acta*, *65*(19), 3267–3287.

Baines, A. G., M. J. Cheadle, H. J. B. Dick, A. H. Scheirer, B. E. John, N. J. Kusznir, and T. Matsumoto (2007), Evolution of the Southwest Indian Ridge from 55°45′E to 62°E: Changes in plate-boundary geometry since 26 Ma, *Geochem. Geophys. Geosyst.*, *8*, Q06022, doi:10.1029/2006GC001559.

Baines, A. G., M. J. Cheadle, B. E. John and J. J. Schwartz (2008), The rate of detachment faulting at an oceanic core complex; Atlantis Bank, SW Indian Ridge, *Earth Planet. Sci. Lett.*, *273*(1–2), 105–114, doi:10.1016/j.epsl.2008.06.013.

Behrmann, J. H. (1985), Crystal plasticity and superplasticity in quartzite: A natural example, *Tectonophysics*, *115*, 101–129.

Blackman, D. K., J. R. Cann, B. Janssen, and D. K. Smith (1998), Origin of extensional core complexes: Evidence from the Mid-Atlantic Ridge at Atlantis fracture zone, *J. Geophys. Res.*, *103*, 21,315–21,333.

Blackman, D. K., et al. (2004), Geology of the Atlantis Massif (Mid-Atlantic Ridge, 30°N): Implications for the evolution of an ultramafic oceanic core complex, *Mar. Geophys. Res*., *23*, 443–469.

Blackman, D. K., B. Ildefonse, B. E. John, Y. Ohara, D. J. Miller, C. J. MacLeod, and the Expedition 304/305 Scientists (2006), *Proceedings of the Integrated Ocean Drilling Program, 304/305*, Integrated Ocean Drilling Program Management International, Inc., College Station, TX, doi:10.2204/iodp.proc.304305.2006.

Boschi, C., G. L. Früh-Green, A. Delacour, J. A. Karson, and D. S. Kelley (2006), Mass transfer and fluid flow during detachment faulting and development of an oceanic core complex, Atlantis Massif, (MAR 30°N), *Geochem. Geophys. Geosyst.*, *7*, Q01004, doi:10.1029/2005GC001074.

Brady, R. J. (2002), Very high slip rates on continental extensional faults: New evidence from (U-Th)/He thermochronometry of the Buckskin Mountains, Arizona, *Earth Planet. Sci. Lett.*, *197*, 95–104.

Brichau, S., U. Ring, R. A. Kecthem, A. Carter, D. Stockli, and M. Brunel (2006), Constraining the long-term evolution of the slip rate for a major extensional fault system in the central Aegean, Greece, using thermochronology, *Earth Planet. Sci. Lett.*, *241*, 293–306.

Buck, W. R. (1988), Flexural rotation of normal faults, *Tectonics*, *7*, 959–973.

Buck, W. R., L. L. Lavier, and A. N. B. Poliakov (2005), Modes of faulting at mid-ocean ridges, *Nature*, *434*, 719–723.

Buick, I. S. (1991), The late Alpine evolution of an extensional shear zone, Naxos, Greece, *J. Geol. Soc. London*, *148*, 92–103.

Buick, I. S., and T. J. B. Holland (1989), The P-T-t path associated with crustal extension, Naxos, Greece, in *Evolution of Metamorphic Belts*, *Geol. Soc. Spec. Publ.*, vol. 43, edited by J. S. Daly, R. A. Cliff, and B. W. D. Yardley, pp. 365–369.

Burchfiel, B. C., C. Zhiliang, K. V. Hodges, L. Yuping, L. H. Royden, D. Changrong, and X. Jiene (1992), The south Tibetan detachment system, Himalayan orogen: Extension contemporaneous with and parallel to shortening in an collisional mountain belt, *Spec. Pap. Geol. Soc. Am.*, *269*, 1–41.

Burgmann, R., and G. Dresen (2008), Rheology of the lower crust and upper mantle: Evidence from rock mechanics, geodesy, and field observations, *Annu. Rev. Earth Planet. Sci.*, *36*, 531–567.

Byerlee, J. (1978), Friction of rocks, *Pure Appl. Geophys.*, *116*, 615–626, doi:10.1007/BF00876528.

Campbell-Stone, E., and B. E. John (2002), Temporal changes in deformation mode: From failure to flow in the Colorado River extensional corridor, *Int. Geol. Rev.*, *44*, 515–527.

Campbell-Stone, E., B. E. John, D. A. Foster, J. W. Geissman, and R. F. Livaccari (2000), Mechanisms for accommodation of Miocene extension: Low-angle normal faulting, magmatism, and secondary breakaway faulting in the southern Sacramento Mountains, southeastern California, *Tectonics*, *19*, 566–587.

Canales, J. P., R. S. Detrick, S. M. Carbotte, G. M. Kent, J. B. Diebold, A. Harding, J. Babcock, M. R. Nedimović, and E. van Ark (2005), Upper crustal structure and axial topography at intermediate spreading ridges: Seismic constraints from the southern Juan de Fuca Ridge, *J. Geophys. Res*, *110*, B12104, doi:10.10129/2005/JB003630.

Canales, J. P., B. E. Tucholke, M. Xu, J. A. Collins, and D. L. DuBois (2008), Seismic evidence for large-scale compositional heterogeneity of oceanic core complexes, *Geochem. Geophys. Geosyst.*, *9*, Q08002, doi:10.1029/2008GC002009.

Cann, J. R., D. K., Blackman, D. K. Smith, E. McAllister, B. Janssen, S. Mello, E. Avgerinos, A. R. Pascoe, and J. Escartin (1997), Corrugated slip surfaces formed at North Atlantic ridge-transform intersections, *Nature*, *385*, 329–332.

Cannat, M. (1993), Emplacement of mantle rocks in the seafloor at mid-ocean ridges, *J. Geophys. Res*., *98*, 4163–4172.

Cannat, M. (1996), How thick is the magmatic crust at slow spreading oceanic ridges, *J. Geophys. Res.*, *101*, 2847–2857.

Cannat, M., C. Mevel, and D. Stakes (1991), Normal ductile shear zones at an oceanic spreading ridge: Tectonic evolution of Site 735 gabbros (southwest Indian Ocean), *Proc. Ocean Drill. Program Sci. Results*, *118*, 415–430.

Cannat, M., D. Sauter, V. Mendel, E. Ruellan, K. Okino, J. Escartin, V. Combier, and M. Baala (2006), Modes of seafloor generation at a melt-poor ultra-slow spreading ridge, *Geology*, *34*, 605–608.

Carter, T .J., B. P., Kohn, D. A. Foster, A. J. W. Gleadow (2004), How the Harcuvar Mountains metamorphic core complex became cool: Evidence for apatite (U-Th)/He thermochronology, *Geology*, *32*, 985–988, doi:10.1130.G20936.1.

Carter, T. J., B. P., Kohn, D. A. Foster, and A. J. W. Gleadow, and J. D. Woodhead (2006), Late-stage evolution of the Chemehuevi-Sacramento detachment faults from apatite (U-Th)/He thermochronology—Evidence for mid-Miocene accelerated slip, *Geol. Soc. Am. Bull.*, *118*, 689–709.

Chapin, C. E., and J. I. Lindley (1986), Potassium metasomatism of igneous and sedimentary rocks in detachment terranes and other sedimentary basins: Economic implications, in *Frontiers in Geology and Ore Deposits of Arizona and the Southwest*, *Arizona Geol. Soc. Digest*, vol. 16, edited by B. Beatty and P. A. K. Wilkinson, pp. 118–126.

Charlou, J.-L., J.-P. Donval, Y. Fouquet, P. Jean-Baptiste, and N. Holm (2002), Geochemistry of high H_2 and CH_4 vent fluids issuing from ultramafic rocks at the Rainbow hydrothermal field (36°14′N, MAR), *Chem. Geol.*, *191*, 345–359.

Cochran, J. R. (2005), Northern Red Sea: Nucleation of an oceanic spreading center within a continental rift, *Geochem. Geophys. Geosyst.*, *6*, Q03006, doi:10.1029/2004GC000826.

Colletta, B., P. LeQuellec, J. Letouzey, and I. Moretti (1988), Longitudinal evolution of the Suez rift structure (Egypt), *Tectonophysics*, *53*, 221–233.

Collettini, C., and R. H. Sibson (2001), Normal faults, normal friction?, *Geology*, *29*, 927–930.

Coogan, L. A., R. N. Wilson, K. M. Gillis, and C. J. MacLeod (2001), Near-solidus evolution of oceanic gabbros: Insights from amphibole geochemistry, *Geochim. Cosmochim. Acta*, *65*, 4339–4357, doi:10.1016/S0016-7037(01)00714-1.

Cowan, D. S., T. T. Cladouhos, and J. K. Morgan (2003), Structural geology and kinematic history of rocks formed along low-angle normal faults, Death Valley, California, *Geol. Soc. Am. Bull.*, *115*, 1230–1248.

Crittenden, M. D., P. J., Coney, and G. H. Davis (1980), Cordilleran metamorphic core complexes, *Mem. Geol. Soc. Am.*, *153*, 490.

Davis, G. A., J. L. Anderson, E. G. Frost, and T. J. Shackleford (1980), Mylonitization and detachment faulting in the Whipple-Buckskin-Rawhide Mountains terrane, southeastern California and western Arizona, in *Cordilleran Metamorphic Core Complexes*, *Mem. Geol. Soc. Am.*, vol. 153, edited by M. D. Crittenden Jr. et al., pp. 79–129.

Davis, G. H. (1983), Shear zone model for the evolution of metamorphic core complexes, *Geology*, *11*, 342–347.

Davis, G. H., and P. J. Coney (1979), Geologic development of Cordilleran metamorphic core complexes, *Geology*, *7*, 120–124.

deMartin, B. J., R. A. Sohn, J. P. Canales, and S. E. Humphris (2007), Kinematics nd geometry of active detachment faulting beneath the Trans-Atlantic geotraverse (TAG) hydrothermal field on the Mid-Atlantic Ridge, *Geology*, *35*, 711–714, doi:10.1130/G23718A.

Dick, H. J. B., H. Schouten, P. S. Meyer, D. G. Gallo, H. Bergh, R. Tyce, P., Patriat, K. T. M. Johnson, J. E. Snow, and A. Fisher (1991), Tectonic evolution of the Atlantis II Fracture Zone, *Proc. Ocean Drill. Program Sci. Results*, *118*, 359–398.

Dick, H. J. B., S. Arai, G. Hirth, B. John, and KR00-06 Scientific Party (2000a), A subhorizontal cross-section through the crust-mantle boundary at the SW Indian Ridge, *Geophys. Res. Abstr.*, *3*.

Dick, H. J. B., et al. (2000b), A long in situ section of lower oceanic crust: Results of ODP Leg 176 drilling at the Southwest Indian Ridge, *Earth Planet. Sci. Lett.*, *179*, 31–51.

Dick, H. J. B., M. A. Tivey, and B. E. Tucholke (2008), Plutonic foundation of a slow-spreading ridge segment: Oceanic core complex at Kane megamullion, 23°30′N, 45°20′W, *Geochem. Geophys. Geosyst.*, *9*, Q05014, doi:10.1029/2007GC001645.

Dimanov, A., and G. Dresen (2005), Rheology of synthetic anorthite-diopside aggregates: Implications for ductile shear zones, *J. Geophys. Res.*, *110*, B07203, doi:10.1029/2004JB003431.

Douville, E., J. L. Charlou, E. H. Oelkers, P. Bienvenu, C. F. Jove Colon, J. P. Donval, Y. Fouquet, D. Prieur, and P. Appriou (2002), The Rainbow vent fluids (36°4′N, MAR): The influence of ultramafic rocks and phase separation on trace metal content in Mid-Atlantic Ridge hydrothermal fluids, *Chem. Geol.*, *184*, 37–48.

Escartin, J., G. Hirth, and B. Evans (1997), Effects of serpentinization on the lithospheric strength and style of normal faulting at slow spreading ridges, *Earth Planet. Sci. Lett.*, *151*, 181–189.

Escartín, J., C. Mével, C. J. MacLeod, and A. M. McCaig (2003), Constraints on deformation conditions and the origin of oceanic detachments: The Mid-Atlantic Ridge core complex at 15°45′N, *Geochem. Geophys. Geosyst.*, *4*(8), 1067, doi:10.1029/2002GC000472.

Escartín, J., D. K. Smith, J. Cann, H. Schouten, C. H. Langmuir, and S. Escrig (2008), Central role of detachment faults in accretion of slow-spreading oceanic lithosphere, *Nature*, *455*, 790–794, doi:10.1038/nature07333.

Foster, D. A., and B. E. John (1999), Quantifying tectonic exhumation in an extensional orogen with thermochronology: Examples from the southern Basin and Range Province, in *Exhumation Processes: Normal Faulting, Ductile Flow, and Erosion*, *Geol. Soc. Spec. Publ.*, vol. 154, edited by U. Ring, M. Brandon, and G. S. Lister, pp. 356–378.

Francis, T. J. G. (1981), Serpentinization faults and their role in the tectonics of slow spreading ridges, *J. Geophys. Res.*, *86*, 11,616–11,622.

Froiztheim, N., and G. Manatschal (1996), Kinematics of Jurassic rifting, mantle exhumation and passive margin formation in the Austroalpine and Peninic nappes (eastern Switzerland), *Geol. Soc. Am. Bull.*, *108*, 1120–1133.

Fujiwara, T., J. Lin, T. Matsumoto, P. B. Kelemen, B. E. Tucholke, and J. F. Casey (2003), Crustal evolution of the Mid-Atlantic Ridge near the Fifteen-Twenty Fracture Zone in the last 5 Ma, *Geochem. Geophys. Geosyst.*, *4*(3), 1024, doi:10.1029/2002GC000364.

Gao, Y., J. Hoefs, R. Przybilla, and J. E. Snow (2006), A complete oxygen isotope profile through the lower oceanic crust, ODP Hole 735B, *Chem. Geol.*, *233*, 217–234.

Garces, M., and J. S. Gee (2007), Paleomagnetic evidence of large footwall rotations associated with low-angle normal faults at the Mid-Atlantic Ridge, *Geology*, *35*, 279–282.

German, C. R., and J. Lin (2004), The thermal structure of the oceanic crust, ridge-spreading and hydrothermal circulation: How well do we understand their inter-connections, in *Mid-ocean Ridges: Hydrothermal Interactions between the Lithosphere and Oceans*, *Geophys. Monogr. Ser.*, vol. 148, edited by C. German, J. Lin, and L. M. Parson, pp. 111–149, AGU, Washington, D. C.

Gràcia, E. J., L. Charlou, J. R. Radford-Knoery, and L. M. Parson (2000), Non-transform offsets along the Mid-Atlantic Ridge south of the Azores (38°N–34°N): Ultramafic exposures and hosting of hydrothermal vents, *Earth Planet. Sci, Lett.*, *177*, 89–103.

Grimes, C. B., B. E. John, M. J. Cheadle, and J. L. Wooden (2008), Protracted construction of gabbroic crust at a slow spreading ridge: Constraints from $^{206}Pb/^{238}U$ zircon ages from Atlantis Massif and IODP Hole U1309D (30ºN, MAR), *Geochem. Geophys. Geosyst.*, *9*, Q08012, doi:10.1029/2008GC002063.

Halfkenny, R. D., R. Kerrich, and W. A. Rehrig (1989), Geology and mineral resources of the Buckskin and Rawhide Mountains, west-central Arizona, *Ariz. Geol. Surv. Bull.*, *198*, 190 pp.

Handy, M., G. Hirth, and R. Brugmann (2007), Continental fault structure and rheology from friction-to-viscous transition downward, in *Tectonic Faults—Agents of Change on a Dynamic Planet*, edited by M. Handy, G. Hirth, and N. Hovius, pp. 139–181, MIT Press, Cambridge, MA.

Hansen, L. (2007), Styles of detachment faulting at the Kane fracture zone oceanic core complex, 23°N mid-Atlantic Ridge, unpublished MS thesis, 116 pp., Univ. of Wyoming, Laramie, WY.

Harigane, Y., K. Michibayashi, and Y. Ohara (2008), Shearing within lower crust during progressive retrogression: Structural analysis of gabbroic rocks from the Godzilla Mullion, an oceanic core complex in the Parece Vela backarc basin, Philippine Sea, *Tectonophysics*, *457*, 183–196.

Hayman, N. W., J. Knott, D. S. Cowan, E. Nemser, and A. M., Sarna-Wojcicki (2003), Quaternary low-angle slip on detachment faults in Death Valley, California, *Geology*, *31*, 343–346.

Hill, E. J., S. L. Baldwin, and G. S. Lister (1995), Magmatism as an essential driving force for formation of active metamorphic core complexes in eastern Papua New Guinea, *J. Geophys. Res.*, *100*, 10,441–10,452.

Hirth, G., C. Teyssier, and W. J. Dunlap (2001), An evaluation of quartzite flow laws based on comparisons between experimentally and naturally deformed rocks, *Int. J. Earth Sci.*, *90*, 77–87.

Holk, G. J., and H. P. Taylor Jr. (2007), $^{16}O/^{18}O$ Evidence for contrasting hydrothermal regimes involving magmatic and meteoric-hydrothermal waters at the Valhalla metamorphic core complex, British Columbia, *Econ. Geol.*, *102*, 1063–1078.

Hollocher, K., J. Spencer, and J. Ruiz (1994), Composition changes in an ash flow cooling unit during K-Metasomatism, west-central Arizona, *Econ. Geol.*, *89*, 877–888.

Hopkinson, L., J. S. Beard, and C. Boulter (2004), The hydrothermal plumbing of a serpentinite-hosted detachment: Evidence from the West Iberia non-volcanic rifted continental margin, *Mar. Geol.*, *204*, 301–315.

Howard, K. A. (1980), Metamorphic infrastructure in the northern Ruby Mountains, Nevada, in *Cordilleran Metamorphic Core Complexes*, *Geol. Soc. Am. Mem.* vol. 153, edited by M. D. Crittenden Jr., P. J. Coney, and G. H. Davis, pp. 335–347.

Howard, K. A. (2003), Crustal structure in the Elko-Carlin Region, Nevada, during Eocene gold mineralization: Ruby-East Humboldt metamorphic core complex as a guide to the deep crust, *Econ. Geol.*, *98*, 240–268.

Howard, K. A., and D. A. Foster (1996), Thermal and unroofing history of a thick, tilted Basin-and-Range crustal section in the Tortilla Mountains, Arizona, *J. Geophys. Res.*, *101*, 511–522.

Howard, K. A., and B. E. John (1987), Crustal extension along a rooted system of imbricate low-angle faults: Colorado River extensional corridor, California and Arizona, in *Continental Extensional Tectonics*, *Geol. Soc. Spec. Publ.*, vol. 28, edited by M. P. Coward, J. F. Dewey, and P. L. Hancock, pp. 299–311.

Ildefonse, B., D. K. Blackman, B. E. John, Y. Ohara, D. J. Miller, C. J. MacLeod, and Integrated Ocean Drilling Program Expeditions 304/305 Science Party (2007), Oceanic core complexes and crustal accretion at slow-spreading ridges, *Geology*, *35*, 623–626.

Jackson, J. A., and N. J. White (1989), Normal faulting in the upper continental crust: Observations from regions of active extension, *J. Struct. Geol.*, *11*, 15–36.

Jansen, J. B. H., and R. D. Schuling (1976), Metamorphism on Naxos; petrology and geothermal gradients, *Am. J. Sci.*, *276*, 1225–1253.

John, B. E. (1987a), Geometry and evolution of a mid-crustal extensional fault system: Chemehuevi Mountains, southeastern California, *Geol. Soc. London Spec. Pap.*, *28*, 313–335.

John, B. E. (1987b), Geologic map of the Chemehuevi Mountains area, San Bernardino County, California, and Mohave County, Arizona, *U.S. Geol. Surv. Open File Rep. 87-666*.

John, B. E., and M. J. Cheadle (2005), Are oceanic detachment faults really analogous to those on the continents?, *Eos Trans. AGU*, *86*(52), Abstract T34B-01.

John, B. E., and D. A. Foster (1993), Structural and thermal constrains on the initiation angle of detachment faulting in the southern Basin and Range: The Chemehuevi Mountains case study, *Geol. Soc. Am. Bull.*, *105*, 1091–1108.

John, B. E., and K. A. Howard (1995), Rapid extension recorded by cooling-age patterns and brittle deformation, Naxos, Greece, *J. Geophys. Res.*, *101*, 9969–9980.

John, B. E., D. A. Foster, J. M. Murphy, M. J. Cheadle, A. G. Baines, C. M. Fanning, and P. Copeland (2004), Determining the cooling history of in suit lower oceanic crust—Atlantis Bank, SW Indian Ridge, *Earth Planet. Sci. Lett*., *222*, 145–160.

Karson, J. A. (1999), Geological investigation of a lineated massif at the Kane transform: Implications for oceanic core complexes, *Philos. Trans. R. Soc. London, Ser. A.*, *357*, 713–740.

Karson, J. A., G. L. Früh-Green, D. S. Kelley, E. A. Williams, D. R. Yorger, and M. Jakuba (2006), Detachment shear zone of the Atlantis Massif core complex, mid-Atlantic Ridge, 30°N, *Geochem. Geophys. Geosyst.*, *7*, Q06016, doi:10.1029/2005GC001109.

Kelemen, P. B., E. Kikawa, D. J. Miller, and Shipboard Scientific Party (2004), *Proc. Ocean Drill. Program Initial Rep. 209*, Ocean Drill. Program, College Station, TX, doi:10.2973/odp.proc.ir.209.2004.

Kelemen, P. B., E. Kikawa, and D. J. Miller (2007), *Proc. Ocean Drill. Program, Sci. Results 209*, Ocean Drill. Program, College Station, TX, doi:10.2973/odp.proc.sr.209.

Kelley, D. S., et al. (2001), An off-axis hydrothermal vent field near the Mid-Atlantic Ridge at 30°N, *Nature*, *412*, 145–149.

Kerrich, R. (1988), Detachment zones of Cordilleran metamorphic core complexes: Thermal, fluid and metasomatic regimes, *Int. J. Earth Sci*., *77*, 157–182, doi:10.1007/BF01848682.

Kohlstedt, D. L., B. Evans, and S. J. Mackwell (1995), Strength of the lithosphere: Constraints imposed by laboratory experiments, *J. Geophys. Res*., *100*, 17,587–17,602, doi:10.1029/95JB01460.

Kong, L. S. L., S. C. Solomon, and G. M. Purdy (1992), Microearthquake characteristics of a mid-ocean ridge along-axis high, *J. Geophys. Res.*, *97*, 1659–1685.

Lavier, L. L., W. R. Buck, and A. N. B. Poliakov (1999), Self-consistent rolling hinge model for the evolution of large offset low-angle normal faults, *Geology*, *27*, 1127–1130.

Lister, G. S., and S. L. Baldwin (1993), Plutonism and the origin of metamorphic core complexes, *Geology*, *21*, 607–610.

Lister, G. S., and G. A. Davis (1989), The origin of metamorphic core complexes and detachment faults formed during Tertiary continental extension in the northern Colorado River region, U.S.A., *J. Struct. Geol.*, *11*, 65–94.

Lister, G. S., M. A. Etheridge, and P. A. Symonds (1991), Detachment models for the formation of passive continental margins, *Tectonics*, *10*, 1038–1064.

Little, T. A., S. L. Baldwin, P. G. Fitzgerald, and B. Monteleone (2007), Continental rifting and metamorphic core complex formation ahead of the Woodlark spreading ridge, D'Entrecasteaux Islands, Papua New Guinea, *Tectonics*, *26*, TC1002, doi:10.1029/2005TC001911.

Losh, S. (1997), Stable isotope and modeling studies of fluid-rock interaction associated with the Snake Range and Mormon peak detachment faults, Nevada, *Geol Soc. Am. Bull.*, *109*, 300–323.

MacLeod, C. J., et al. (2002), Direct geological evidence for oceanic detachment faulting: The Mid-Atlantic Ridge 15°45′N, *Geology*, *30*, 879–882.

Maeda, J. (2002), High-temperature fluid migration within oceanic Layer 3 gabbros, Hole 735B, Southwest Indian Ridge: Implications for magmatic-hydrothermal transition at slow-spreading mid-ocean ridges, in *Proc. Ocean Drill. Program Sci. Results*, vol. 176, edited by J. H. Natland et al., pp. 1–56, Ocean Drill. Program, College Station, TX.

Manning, C. E., P. Weston, and K. I. Mahon (1996), Rapid high-temperature metamorphism of East Pacific Rise gabbros from Hess Deep, *Earth Planet. Sci. Lett.*, *144*, 123–132, doi:10.1016/0012-821X(96)00153-7.

Matsumoto, T., H. J. B. Dick, and S. S. Party (2002), *Preliminary Report (ABCDE) Yokosuka/Shinkai 6500 YK01-14 Cruise Results*, Japan Marine Science and Technology Center, Yokosuka-City, Kanagawa, Japan.

McCaig, A. M., R. A. Cliff, J. Escartin, A. E. Fallick, and C. J. MacLeod (2007), Oceanic detachment faults focus very large volumes of black smoker fluids, *Geology*, *35*, 935–938.

McCaig, A. M., A. Delacour, A. E. Fallick, T. Castelain, and G. L. Früh-Green (2010), Detachment fault control on hydrothermal circulation systems: Interpreting the subsurface beneath the TAG hydrothermal field using the isotopic and geological evolution of oceanic core complexes in the Atlantic, in *Diversity of Hydrothermal Systems on Slow Spreading Ocean Ridges, Geophys. Monogr. Ser*., doi:10.1029/2008GM000729, this volume.

Mehl, L., and G. Hirth (2008), Plagioclase preferred orientation in layered mylonites: Evaluation of flow laws for the lower crust, *J. Geophys. Res.*, *113*, B05202, doi:10.1029/2007JB005075.

Michael, P., et al. (2003), Magmatic and amagmatic seafloor generation at the ultraslow spreading Gakkel Ridge, Arctic Ocean, *Nature*, *423*, 956–961.

Michalski, J. R., S. J. Reynolds, P. B. Niles, T. G. Sharp, and P. R. Christensen (2007), Alteration mineralogy in detachment zones: Insights from Swansea, *Geosphere*, *3*, 184–198.

Miller, E. L., T. A. Dumitru, R. W. Brown, and P. B. Gans (1999), Rapid Miocene slip on the Snake Range-Deep Creek Range fault system, east-central Nevada, *Geol. Soc. Am. Bull.*, *111*, 886–905.

Miller, J. M. G., and B. E. John (1988), Detached strata in a Tertiary low-angle normal fault terrane, southeastern California: A sedimentary record of unroofing, breaching, and continued slip, *Geology*, *19*, 645–648.

Miranda, E. A. (2006), Structural development of the Atlantis Bank Oceanic Detachment faults system, Southwest Indian Ridge; unpublished PhD dissertation, 441 pp., Univ. of Wyoming, Laramie, WY.

Miranda, E. A., and B. E. John (2010), Strain localization along the Atlantis Bank oceanic detachment fault system, Southwest Indian Ridge, *Geochem. Geophys. Geosyst., 11*, Q04002, doi: 10.1029/2009GC002646.

Miranda, E. A., B. E. John, and B. R. Frost (2003), Oceanic core complex development within the ductile and brittle regimes, Atlantis Bank, Southwest Indian Ridge, *Eos Trans. AGU*, *84*(46), Fall Meet. Suppl., Abstract V21D-0555.

Morris, A., J. S. Gee, N. Pressling, B. E. John, C. J. MacLeod, C. B. Grimes, and R. C. Searle (2009), Footwall rotation in an oceanic core complex quantified using reoriented Integrated Ocean Drilling Program core samples, *Earth Planet. Sci. Lett., 287*, 217–228, doi:10.1016/j.epsl.2009.08.007/.

Morrison, J. (1994), Downward circulation of meteoric water into the lower-plate of the Whipple Mountains metamorphic core complex, California, *J. Metamorph. Geol.*, *12*, 827–840.

Morrison, J., and J. L. Anderson (1998), Footwall refrigeration along a detachment fault: Implications for the thermal evolution of core complexes, *Science*, *279*, 63–66.

Morton, J. L., and N. H. Sleep (1985), A mid-ocean ridge thermal model: Constraints on the volume of axial hydrothermal heat flux, *J. Geophys. Res.*, *90*, 11,345–11,353.

Natland, J., P. S. Meyer, H. J. B. Dick, and S. H. Bloomer (1991), Magmatic oxides and sulfides in gabbroic rocks from ODP Hole 735B and the later development of the liquid line of descent, in *Proc. Ocean Drill. Program, Sci. Results*, vol. 118, edited by R. P. Von Herzen et al., pp. 75–112, Ocean Drill. Program, College Station, TX.

Numelin, T., E. Kirby, J. D. Walker, and B. Didericksen (2007a), Late Pleistocene slip on a low-angle normal fault, Searles Valley, California, *Geosphere*, *3*, 163–176.

Numelin, T., C. Marone, and E. Kirby (2007b), Frictional properties of natural fault gauge from a low-angle normal fault, Panamint Valley, California, *Tectonics*, *26*, TC2004, doi:10.1029/2005TC001916.

Ohara, Y., T. Yoshida, Y. Kato, and S. Kasuga (2001), Giant megamullion in the Parece Vela backarc basin, *Mar. Geophys. Res.*, *22*, 47–61.

Okino, K., K. Matsuda, D. M. Christie, Y. Nogi, and K. Koizumi (2004), Development of oceanic detachment and asymmetric spreading at the Australian-Antarctic Discordance, *Geochem. Geophys. Geosyst.*, *5*, Q12012, doi:10.1029/2004GC000793.

Perez-Gussinye, M., and T. J. Reston (2001), Rheological evolution during extension at nonvolcanic rifted margins: Onset of serpentinization and development of detachments leading to continental break-up, *J. Geophys. Res.*, *106*, 3961–3975.

Person, M., A. Mulch, C. Teyssier, and Y. Gao (2007), Isotope transport and exchange within metamorphic core complexes, *Am. J. Sci*., *307*, 555–589.

Phipps-Morgan, J., and Y. J. Chen (1993), The genesis of oceanic crust: Magma injection, hydrothermal circulation, and crustal flow, *J. Geophys. Res.*, *98*, 6283–6297.

Proffett, J. M., Jr. (1977), Cenozoic geology of the Yerington District, Nevada, and implications for the nature and origin of Basin and Range faulting, *Geol. Soc. Am. Bull.*, *88*, 247–266.

Reinen, L. A. (2000), Seismic and aseismic slip indicators in serpentinite gouge, *Geology*, *28*, 135–138.

Reynolds, S. J. (1985), Geology of the south mountains, central Arizona, *Ariz. Bur. Geol. Miner. Technol. Bull.*, *195*, 61 pp.

Reynolds, S. J., and G. S. Lister (1987), Structural aspects of fluid-rock interactions in detachment zones, *Geology*, *15*, 362–366.

Reynolds, S. J., and J. E. Spencer (1985), Evidence for large-scale transport on the Bullard detachment fault, west-central Arizona, *Geology*, *13*, 353–356.

Richard, S. M., J. E. Fryxell, and J. E. Sutter (1990), Tertiary structure and thermal history of the Harquahala and Buckskin Mountains, west-central Arizona: Implications for denudation by a major detachment fault system, *J. Geophys. Res.*, *95*, 19,973–19,987.

Robinson, P. T., J. Erzinger, and R. Emmermann (2002), The composition and origin of igneous and hydrothermal veins in the lower ocean crust—ODP Hole 735B, Southwest Indian Ridge, in *Proc. Ocean Drill. Program Sci. Results*, vol. 176, edited by J. H. Natland et al., Ocean Drill. Program, College Station, TX.

Roddy, M. S., S. J. Reynolds, B. M. Smith, and J. Ruiz (1988), K-metasomatism and detachment-related mineralization, Harcuvar Mountains, Arizona, *Geol. Soc. Am. Bull.*, *100*, 1627–1639.

Rybacki, E., and G. Dresen (2000), Dislocation and diffusion creep of synthetic anorthite aggregates, *J. Geophys. Res.*, *15*, 26,017–26,036.

Rybacki, E., and G. Dresen (2004), Deformation mechanism maps for feldspar rocks, *Tectonophysics*, *382*, 173–187, doi:10.1016/j.tecto.2004.01.006.

Scholz, C. H. (2002), *The Mechanics of Earthquakes and Faulting*, 471 pp., Cambridge Univ. Press, New York.

Schroeder, T., and M. J. Cheadle (2007), What is an oceanic core complex?, *Eos Trans. AGU*, *88*(52), Abstract T53B-1293.

Schroeder, T., and B. E. John (2004), Strain localization on an oceanic detachment fault system, Atlantis Massif, 30°N, Mid-Atlantic Ridge, *Geochem. Geophys. Geosyst.*, *5*, Q11007, doi:10.1029/2004GC000728.

Schroeder, T., B. E. John, and B. R. Frost (2002), Geologic implications of seawater circulation through peridotite exposed at slow spreading mid-ocean ridges, *Geology*, *30*, 367–370.

Schroeder, T., M. J. Cheadle, H. J. B. Dick, U. Faul, J. F. Casey, and P. B. Kelemen (2007), Nonvolcanic seafloor spreading and corner-flow rotation accommodated by extensional faulting at 15°N on the Mid-Atlantic Ridge: A structural synthesis of ODP Leg 209, *Geochem. Geophys. Geosyst.*, *8*, Q06015, doi:10.1029/2006GC001567.

Schulz, N. J., R. S. Detrick, and S. P. Miller (1988), Two- and three-dimensional inversions of magnetic anomalies in the MARK Area (Mid-Atlantic Ridge 23°N), *Mar. Geophys. Res.*, *10*, 41–57, doi:10.1007/BF02424660.

Schwartz, J. J., B. E. John, M. J. Cheadle, E. A. Miranda, C. B. Grimes, J. L. Wooden, and H. J. B. Dick (2005), Dating the growth of oceanic crust at a slow-spreading ridge, *Science*, *310*, 654–657.

Schwartz, J. J., B. E. John, M. J. Cheadle, P. W. Reiners, and A. G. Baines (2009), Cooling history of Atlantis Bank oceanic core complex: Evidence for hydrothermal activity 2.6 Ma off axis, *Geochem. Geophys. Geosyst.*, *10*, Q08020, doi:10.1029/2009GC002466.

Searle, R. C., M. Cannat, K. Fujioka, C. Mével, H. Fujimoto, A. Bralee, and L. Parson (2003), FUJI Dome: A large detachment fault near 64°E on the very slow-spreading Southwest Indian Ridge, *Geochem. Geophys. Geosyst.*, *4*(8), 9105, doi:10.1029/2003GC000519.

Shipboard Scientific Party (1999), Leg 176 Summary, in *Proc. Ocean Drill. Program, Initial Rep.*, vol. 176, edited by H. J. B. Dick et al., pp. 1–70, Ocean Drill. Program, College Station, TX, doi:10.2973/odp.proc.ir.176.101.1999.

Sibson, R. H. (1977), Fault rocks and fault mechanisms, *J. Geol. Soc. London*, *133*(3), 191–213, doi:10.1144/gsjgs.133.3.0191.

Sibson, R. H. (1985), A note on fault reactivation, *J. Struct. Geol.*, *7*, 751–754.

Sibson, R. H. (2000), Fluid involvement in normal faulting, *J. Geodyn.*, *29*, 469–499.

Smith, D. K., J. R. Cann, and J. Escartin (2006), Widespread active detachment faulting and core complex formation near 13°N on the mid-Atlantic Ridge, *Nature*, *442*, 440–443.

Smith, D. K., J. Escartin, H. Schouten, and J. R. Cann (2008), Fault rotation and core complex formation: Significant processes in seafloor formation at slow-spreading mid-ocean ridges (Mid-Atlantic Ridge, 13°–15°N), *Geochem. Geophys. Geosyst.*, *9*, Q03003, doi:10.1029/2007GC001699.

Sonder, J. J., and C. H. Jones (1999), Western United States: How the West was widened, *Annu. Rev. Earth Planet. Sci.*, *27*, 417–462.

Spell, T. L., I. McDougall, and A. J. Tulloch (2000), Thermochronologic constraints on the breakup of the Pacific Gondwana margin: The Paparoa metamorphic core complex, South Island, New Zealand, *Tectonics*, *19*, 433–451.

Spencer, J. E. (1984), The role of tectonic denuation in the warping and uplift of low-angle normal faults, *Geology*, *12*, 95–98.

Spencer, J. E. (1999), Geologic continuous casting below continental detachment faults and at the striated extrusion of Sacsayhuaman, Peru, *Geology*, *27*, 327–330.

Spencer, J. E., and J. W. Welty (1986), Possible controls of base- and precious-metal mineralization associated with Tertiary detachment faults in the lower Colorado River trough, Arizona and California, *Geology*, *14*, 195–198.

Stakes, D., C. Mevel, M. Cannat, and T. Chaput (1991), Metamorphic stratigraphy of Hole 735B, *Proc. Ocean Drill. Program Sci. Results*, *118*, 153–180.

Swift, S. A., H. Hoskins, and R. A. Stephen (1991), Seismic stratigraphy in a transverse ridge, Atlantis II Fracture Zone, in *Proc. Ocean Drill. Program Sci. Results*, vol. 118, edited by R. P. Von Herzen et al., pp. 219–226, Ocean Drill. Program, College Station, TX.

Talbot, C. J., and W. Ghebreab (1997), Red Sea detachment and basement core complexes in Eritrea, *Geology*, *25*, 655–658.

Teyssier, C., E. Ferré, D. L. Whitney, B. Norlander, O. Vanderhaeghe, and D. Parkinson (2005), Flow of partially molten crust and origin of detachments during collapse of the Cordilleran orogen, in Bruhn, D. and Burlini, L. (eds.), High-Strain Zones: Structure and Physical Properties, *Geol. Soc. Spec. Publ.*, *245*, 39–64.

Tivey, M. A., H. Schouten, and M. C. Kleinrock (2003), A near-bottom magnetic survey of the Mid-Atlantic Ridge axis at 26°N: Implications for the tectonic evolution of the TAG segment, *J. Geophys. Res.*, *108*(B5), 2277, doi:10.1029/2002JB001967.

Toomey, D., S. C. Solomon, and G. M. Purdy (1988), Mircoearthquakes beneath the median valley of the Mid-Atlantic Ridge near 23°N: Tomography and tectonics, *J. Geophys. Res.*, *93*, 9093–9112.

Tucholke, B. E., J. Lin, and M. C. Kleinrock (1998), Megamullions and mullion structure defining oceanic metamorphic core complexes on the Mid-Atlantic Ridge, *J. Geophys. Res.*, *103*, 9857–9866.

Tucholke, B. E., M. D. Behn, W. R. Buck, and J. Lin (2008), Role of melt supply in oceanic detachment faulting and formation of megamullions, *Geology*, *36*, 455–458.

Vanko, D. A., and D. S. Stakes (1991), Fluids in ocean layer 3: Evidence from veined rocks, Hole 745B, Southwest Indian Ridge, *Proc. Ocean Drill. Program Sci. Results*, *118*, 181–215.

Wernicke, B. (1981), Low-angle normal faults in the Basin and Range province: Nappe tectonics in an extending orogen, *Nature*, *291*, 645–648.

Wernicke, B. (1992), Cenozoic extensional tectonics of the U.S. Cordillera, in *The Cordilleran Orogen: Conterminous U.S., The Geology of North America, G-3*, edited by B. C. Burchfiel, P. W. Lipman, and M. L. Zoback, pp. 553–582, Geol. Soc. Am., Boulder, Colorado.

Wernicke, B. (1995), Low-angle normal faults and seismicity: A review, *J. Geophys. Res.*, *100*, 20,159–20,174.

Wernicke, B., and G. J. Axen (1988), On the role of isostasy in the evolution of normal fault systems, *Geology*, *16*, 848–851.

Whitney, D. L., C. Teyssier, and M. T. Heizler (2007), Gneiss domes, metamorphic core complexes, and wrench zones: Thermal and structural evolution of the Niğde Massif, central Anatolia, *Tectonics*, *26*, TC5002, doi:10.1029/2006TC002040.

Wilkins, J., Jr., R. E. Beane, and T. L. Heidrick, (1986), Mineralization related to detachment faults: A model, in *Frontiers in Geology and Ore Deposits of Arizona and the Southwest*, *Arizona Geol. Soc. Digest*, vol. 16, edited by B. Beatty and P. A. K. Wilkinson, pp. 108–117.

Williams, C. M. (2007), Oceanic lithosphere magnetization: Marine magnetic investigations of crustal accretion and tectonic processes in mid-ocean ridge environments, Ph.D. thesis, 285 pp., Mass. Inst. of Technol., Woods Hole Oceanogr. Inst., Woods Hole, MA.

Worm, H. U. (2001), Magnetic stability of oceanic gabbros from ODP Hole 735B, *Earth Planet. Sci. Lett.*, *193*, 287–302.

Yin, A., and J. F. Dunn (1992), Structural and stratigraphic development of the Whipple-Chemehuevi detachment fault system, southeastern California: Implications for the geometrical evolution of domal and basinal low-angle normal faults, *Geol. Soc. Am. Bull.*, *104*, 659–674.

M. J. Cheadle and B. E. John, Department of Geology and Geophysics, University of Wyoming, Laramie, WY 82070, USA. (bjohn@uwyo.edu)